

Spin-liquid states on the triangular and Kagomé lattices: A projective-symmetry-group analysis of Schwinger boson states

Fa Wang¹ and Ashvin Vishwanath^{1,2}¹*Department of Physics, University of California, Berkeley, California 94720, USA*²*Materials Sciences Division, Lawrence Berkeley National Laboratory, Berkeley, California 94720, USA*

(Received 15 August 2006; published 21 November 2006)

A symmetry-based analysis (projective symmetry group) is used to study spin-liquid phases on the triangular and Kagomé lattices in the Schwinger boson framework. A maximum of eight distinct Z_2 spin-liquid states are found for each lattice, which preserve all symmetries. Out of these only a few have nonvanishing nearest-neighbor amplitudes, which are studied in greater detail. On the triangular lattice, only two such states are present—the first (zero-flux state) is the well-known state introduced by Sachdev, which on condensation of spinons leads to the 120° ordered state. The other solution, which we call the π -flux state has not previously been discussed. Spinon condensation leads to an ordering wave vector at the Brillouin zone edge centers, in contrast to the 120° state. While the zero-flux state is more stable with just nearest-neighbor exchange, we find that the introduction of either next-neighbor antiferromagnetic exchange or four-spin ring exchange (of the sign obtained from a Hubbard model) tends to favor the π -flux state. On the Kagomé lattice four solutions are obtained—two have been previously discussed by Sachdev, which on spinon condensation give rise to the $q=0$ and $\sqrt{3}\times\sqrt{3}$ spin-ordered states. In addition we find two states with significantly larger values of the quantum parameter at which magnetic ordering occurs. For one of them this even exceeds unity $\kappa_c \approx 2.0$ in a nearest-neighbor model, indicating that if stabilized, could remain spin disordered for physical values of the spin. This state is also stabilized by ring-exchange interactions with signs as derived from the Hubbard model.

DOI: [10.1103/PhysRevB.74.174423](https://doi.org/10.1103/PhysRevB.74.174423)

PACS number(s): 75.10.Jm, 71.10.Hf

I. INTRODUCTION

Recent experiments on frustrated quantum magnets with unusual properties¹⁻⁴ has revived interest in spin-liquid phases. At the same time the theoretical understanding of spin-liquid phases in $D > 1$ has also matured over the last few years—for example, it is now established that such states are typically accompanied by emergent gauge fields in their deconfined phase. Simple and tractable lattice Hamiltonians that realize these phases can also be constructed. Nevertheless, there is still a pressing need to understand the situations in which microscopic spin models might exhibit such phases, and the variety of such phases and their phenomenological properties.

The triangular lattice antiferromagnet has been considered a good place to look for such spin-liquid states. Its geometry is considered less conducive to magnetic order than, for example, the square-lattice antiferromagnet, and more recently there has been evidence from numerical calculations⁵⁻⁸ especially in the presence of anisotropic interactions and ring exchange, for unconventional physics. Similarly, recent experiments on quantum magnets with a triangular lattice structure— Cs_2CuCl_4 ,¹ $\kappa\text{-(ET)}_2\text{Cu(CN)}_3$,² and ^3He films adsorbed on graphite³ show unusual properties that may be interpreted in terms of spin-liquid phases or proximity to such a state. While the spin-gapped Z_2 spin-liquid states considered in this paper are probably not appropriate to directly describe these experimental systems, except perhaps at the very lowest temperatures, they motivate a closer study of possible spin-liquid states on the triangular lattice. The highly frustrated Kagomé lattice has long been considered a good system for realizing exotic ground states. While there are fewer experimentally well-studied examples of quantum

spins on the Kagomé lattice, conventional semiclassical analysis fails to produce a unique ground state when applied to this frustrated lattice. Hence, spin-disordered states such as spin liquids may be realized.

In describing spin-liquid states of quantum magnets, two distinct approaches have been found to be useful. The first involves writing the quantum spin (e.g., spin-1/2) as a fermion bilinear (fermionic spinons), and imposing a constraint on the total number of fermions on each site. This fermionic approach is analytically pursued by writing down a mean-field ansatz where the constraint is imposed only on average to begin with. This mean-field theory may also be viewed as a source of variational wave functions, which after projection yields spin-wave functions. An important step in understanding the variety of spin-liquid states possible in this representation was taken by Wen and collaborators⁹⁻¹¹ who introduced the projective symmetry group (PSG) classification of spin liquids that respect the microscopic symmetries of the system. This provides a guide to identifying the correct gauge group describing the spin liquid (if it survives projection) and also allows for a further classification of different spin-liquid phases with the same gauge group. These different spin-liquid phases differ in subtle ways from one another, for example, in terms of the location of the wave vector of their lowest-energy spin-1 excitation. The advantage of such a classification is that it allows for an exploration of possible spin-liquid states independent of specific Hamiltonians that might realize them as ground states. In this way the symmetric spin-liquid states within the fermionic spin representation on the square and triangular lattices were classified.^{10,11}

A different way to describe spin liquids is via the Schwinger boson approach, where the spin operator is written as a boson bilinear (bosonic spinons) and was analyzed

using a large- N approach.^{12–15} An advantage of this approach is that it is able to readily access both spin-liquid states as well as conventional magnetically ordered states, which arise from the condensation of the Schwinger bosons. For instance, in the case of the triangular lattice,¹⁵ Sachdev found a spin-liquid state, which on decreasing the strength of quantum fluctuations to the size expected for $s=1/2$, gave way to the 120° magnetically ordered state, expected of classical spins on this lattice. However, the possibility of other Schwinger boson spin-liquid states on the triangular lattice have not been systematically explored. Similarly, on the Kagomé lattice, Sachdev¹⁵ found two solutions, which on spinon condensation gives rise to $\sqrt{3} \times \sqrt{3}$ or the $q=0$ magnetically ordered states.

Mapping out the possible spin-liquid states on these lattices is of interest for two reasons. First, when attempting to identify a candidate spin-liquid state to match with experimental data or numerical simulations, one needs to specify precisely what the nature of the state is, and the quantum numbers of its excitations. Therefore while the simplest spin liquid may fail to match these details, other spin-liquid states may give different predictions. Second, there may exist solutions stabilized with different interactions that remain spin liquids even for physical values of the spin. This would be particularly appealing as it would also provide direction to the search for spin-liquid states. Even when the system is in the ordered phase, if it is proximate to a critical point where spin-liquid physics holds, it has been argued¹⁶ that finite-energy and finite-temperature signatures of this will be unusual and best described in terms of the spin-liquid variables. Therefore, a systematic investigation of the possible solutions of the Schwinger boson states is required on the lines of the PSG analysis of the fermionic spin-liquid states. This will also shed light on the connection between two approaches, for example, which states can be described in one but not the other approach.

In this paper we will adapt the technique of projective symmetry Groups, developed by Wen and collaborators^{9–11} in the context of fermionic mean-field theories, to study Schwinger boson mean-field theories. We will focus on the triangular and Kagomé lattices, in particular, on spin-liquid states with the Ising gauge group (Z_2 gauge theories), which preserve the microscopic spin symmetries. Surprisingly, the number is not large (less than or equal to eight for both lattices), which includes, in addition to the solution found by Sachdev, a set of fundamentally different mean-field wave functions, which give rise to Z_2 spin liquids. In particular, if we make the further reasonable assumption of restricting to states with nontrivial nearest-neighbor bond amplitudes, there is only one other state on the triangular lattice, which we call the π -flux state. Similarly, on the Kagomé lattice, Z_2 spin-liquid states with nonvanishing nearest-neighbor bond amplitudes, include, in addition to the two states found by Sachdev, two additional states, which we refer to as the $[\pi \text{ Hex}, \pi \text{ Rhom}]$ and $[0 \text{ Hex}, \pi \text{ Rhom}]$ (which specifies the flux in the length-6 hexagonal loop and the length-8 rhombus). One of the problems in searching for spin-liquid states has been the tendency of various spin Hamiltonians to yield magnetically ordered states, which is reflected in the small values of κ_c , the critical quantum parameter at which spin

ordering occurs in the Sachdev states: $\kappa_c \approx 0.3$ on the triangular and $\kappa_c \approx 0.5$ for the Kagomé states in large N .¹⁵ (Note, $\kappa=2S$ in the case of spin S but it is convenient to extend it to take on all real values.) A feature of the new states is their relative stability against magnetic order, which is seen in the larger critical quantum parameter at which spin ordering occurs: $\kappa_c \approx 0.75$ for the Π -flux triangular state, and $\kappa_c \approx 0.9$ and $\kappa_c \approx 2.0$ for the two new Kagomé states, respectively, in nearest-neighbor models.

While the distinct mean-field solutions of the PSG analysis are typically local minima of the mean-field energy, an important question is whether they can be stabilized as global minima with appropriate interactions. This is discussed in detail for the case of the triangular lattice in this paper. While the zero-flux state is stabilized with just nearest-neighbor antiferromagnetic spin couplings, introducing next-neighbor antiferromagnetic couplings or ring exchange (of the sign arising from the Hubbard model) both tend to favor the π -flux state. We obtain the conditions on the microscopic spin interactions, which favor this state and argue that this may be a fruitful parameter regime for numerical searches for spin liquids. In general, we find that ring exchange on even-length loops (with the sign as derived from the Hubbard model), favors states with π flux on length- $4n$ loops, while it favors states with zero flux in length- $(4n+2)$ loops (n is a positive integer). This is in contrast to a fermionic case where ring exchange disfavors flux¹⁷ for fermions in all loops. Addition of ring exchange on length-6 and length-8 loops can stabilize the $[0 \text{ Hex}, \pi \text{ Rhom}]$ state on the Kagomé, which is a good spin-liquid candidate since it has $\kappa_c=2.0$.

On spinon condensation, the triangular lattice π -flux state naturally leads to magnetically ordered states with wave vectors at the midpoints of the Brillouin zone edges (in contrast to the zero-flux state, which leads to the 120° state with a wave vector at the zone corners). This allows us to understand semiclassical (large spin) calculations in the presence of moderate-neighbor antiferromagnetic couplings or “antiferromagnetic” (with sign as obtained from the Hubbard model) ring exchange on the triangular lattice, where ordered states with the same wave vector are found. It is tempting to connect the possible ordered states on the triangular lattice as emerging from spin condensation out of the few Schwinger boson spin-liquid states allowed by the PSG. New quantum transitions are expected on spinon condensation out of the spin-liquid states obtained here, and will be the subject of future study.

In Sec. II we briefly review the Schwinger boson mean-field theory. Section III analyzes possible spin-liquid states on the triangular lattice. It first reviews the PSG classification of spin-liquid states and the strong constraints that arise from relations between symmetry-group elements. This is then applied to Schwinger boson states on the triangular lattice. A new state is found (the π -flux state) which is further analyzed—in particular, spin configurations resulting from spinon condensation are described, and Hamiltonians stabilizing this mean-field solution are obtained. The general effect of ring-exchange interactions on Schwinger boson mean-field states is discussed. In Sec. VI possible spin-liquid states on the Kagomé lattice are studied, and the properties of one of them, which is unusually stable against spin order-

ing, is described in more detail. The PSG analysis and other details are relegated to the appendixes, which also contain an analysis for other lattices of interest such as the anisotropic triangular lattice.

II. SCHWINGER BOSON MEAN-FIELD THEORY

There are a variety of ways of formulating the Schwinger boson mean-field theory, for example, as a large- N approach^{12,13} or as an approximate variational approach.

Here we will formulate a variational approach that will provide us with a unified way to study the effect of different interactions. We write the spin Hamiltonian,

$$H = J_1 \sum_{\langle ij \rangle} \mathbf{S}_i \cdot \mathbf{S}_j + J_2 \sum_{\langle\langle ij \rangle\rangle} \mathbf{S}_i \cdot \mathbf{S}_j + \dots, \quad (1)$$

in terms of Schwinger bosons,

$$\mathbf{S}_i \cdot \mathbf{S}_j = \frac{1}{4} b_{i\sigma}^\dagger \sigma_{\sigma\sigma'} b_{i\sigma'} b_{j\tau}^\dagger \sigma_{\tau\tau'} b_{j\tau'}, \quad (2)$$

with the constraint that at every site

$$\sum_{\sigma} b_{i\sigma}^\dagger b_{i\sigma} = \kappa, \quad (3)$$

where for a spin system with spin S , $\kappa = 2S$. In the analysis below, it will be convenient to consider κ to be a continuous parameter, taking on any nonnegative value.

We now consider a variational approach to finding the ground states and excitations of Eq. (1). Motivated by the operator identity

$$\mathbf{S}_i \cdot \mathbf{S}_j = : \hat{B}_{ij}^\dagger \hat{B}_{ij} : - \hat{A}_{ij}^\dagger \hat{A}_{ij}, \quad (4)$$

where $: :$ is normal ordering and operators \hat{A} and \hat{B} are defined as

$$\hat{B}_{ij} = \frac{1}{2} \sum_{\sigma} b_{i\sigma}^\dagger b_{j\sigma}, \quad (5)$$

$$\hat{A}_{ij} = \frac{1}{2} \sum_{\sigma, \sigma'} \epsilon_{\sigma\sigma'} b_{i\sigma} b_{j\sigma'}. \quad (6)$$

We consider a “mean-field” Hamiltonian, which is quadratic in terms of the Schwinger bosons,

$$H_{MF} = \sum_{ij} J_{ij} (-A_{ij}^* \hat{A}_{ij} + B_{ij}^* \hat{B}_{ij} + \text{H.c.}) + \sum_{ij} J_{ij} (A_{ij}^* A_{ij} - B_{ij}^* B_{ij}) - \mu \sum_i \left(\sum_{\sigma} b_{i\sigma}^\dagger b_{i\sigma} - \kappa \right), \quad (7)$$

where complex numbers $A_{ij} = -A_{ji}$, $B_{ij} = B_{ji}^*$ are the parameters of the mean-field ansatz.

In the large- N $Sp(N)$ theory, the mean-field Hamiltonian contains only the large- N generalization of the A term. However, since both A and B terms are consistent with global $SU(2)$ symmetry (global spin-rotation symmetry) they are both included in the current theory. The introduction of both terms can be found in Gazza¹⁸ and many other papers.^{19,20}

This Hamiltonian is used to generate a variational wave function in terms of the variational parameters $|\Psi(A_{ij}, B_{ij}, \mu)\rangle$. In order to obtain a spin wave function, we need to project $|\Psi\rangle$ into the constrained Hilbert space where the total number of bosons at each site is exactly $2S$. Strictly speaking, one must evaluate variational energies after this projection step, using the spin Hamiltonian (1). This generalization of Gutzwiller projection to Schwinger boson has been studied by Chen and collaborators.^{21,22} However, since this hard projection is not possible to implement analytically (it is even difficult to do numerically) we rely on an approximate strategy that foregoes implementing the constraint locally, but only on the average—i.e., we tune μ to ensure that

$$\sum_{\sigma} \langle b_{i\sigma}^\dagger b_{i\sigma} \rangle = \kappa. \quad (8)$$

We then evaluate the expectation value of the Hamiltonian (2) written out in terms of Schwinger bosons (2) using the variational wave function. The resulting variational energy is then minimized with respect to the variational parameters A_{ij}, B_{ij} . This yields the self-consistent equations

$$\langle \hat{A}_{ij} \rangle = A_{ij}, \quad \langle \hat{B}_{ij} \rangle = B_{ij}. \quad (9)$$

When these self-consistent equations are satisfied, the variational (mean-field) energy is simply obtained by utilizing the following identity:

$$\langle \mathbf{S}_i \cdot \mathbf{S}_j \rangle = \frac{3}{2} (|B_{ij}|^2 - |A_{ij}|^2). \quad (10)$$

The effect of projection on energetics will be a topic of future study.

III. PSG FOR SCHWINGER BOSON STATES ON THE TRIANGULAR LATTICE

We would like to classify Schwinger boson mean-field states available to us on the triangular lattice in terms of the distinct spin-liquid phases they can give rise to. This exercise allows us to readily obtain potentially interesting states relevant to quantum spin systems on the triangular lattice. Interactions that stabilize these states are discussed subsequently.

This classification follows the classification of fermionic mean-field states in Refs. 9–11. Here however, the underlying local transformation is $U(1)$ (not $SU(2)$ as in the case of fermions). For mean-field theories that survive projection (or equivalently, survive fluctuations) to give rise to a spin-liquid state, this procedure classifies the distinct quantum phases of the system. We will require that the mean-field theory reflects the underlying microscopic symmetries of the spin model. This leads to symmetric spin-liquid states. The symmetry transformations include the space group (lattice translations and point-group symmetries) of the triangular lattice, spin-rotation symmetry, and time-reversal symmetry. The notable ingredient here is that the mean-field state may preserve these symmetries in some indirect way. In addition to the symmetries of the original spin model, one also finds an extra global symmetry in all the mean-field Ansätze which is a subset of the local $U(1)$ transformations mentioned previ-

ously. This is called the invariant gauge group (IGG) in the terminology of Ref. 9. Since we are interested in mean-field states that have exactly the same symmetry as the underlying spin model, not less or more, this is to be identified with the gauge group of the emergent gauge theory. In the examples below we will find an extra Z_2 symmetry in the mean-field Ansatz; hence the spin liquids that are obtained with this procedure are Z_2 spin liquids, but with different internal structures depending on how the microscopic symmetries of the lattice model are realized. Thus, in contrast to conventional states, which are distinguished by patterns of broken symmetry, spin-liquid phases that are completely symmetric and even share the same gauge group can be further distinguished in terms of how the symmetries are realized.

In the Schwinger boson representation of spins, there is a local $U(1)$ transformation of bosons,

$$b_{\mathbf{r}\sigma} \rightarrow e^{i\phi(\mathbf{r})} b_{\mathbf{r}\sigma}, \quad (11)$$

which leaves all physical observables unchanged. Under this transformation, our mean-field ansatz (A_{ij}, B_{ij}) also transform

$$A_{ij} \rightarrow e^{-i\phi(i)-i\phi(j)} A_{ij}, \quad (12a)$$

$$B_{ij} \rightarrow e^{+i\phi(i)-i\phi(j)} B_{ij}. \quad (12b)$$

Two mean-field Ansätze that are related by such a transformation give rise to the same spin-wave function after projection. However, we will be interested in a class of transformations that leave the mean-field Ansatz invariant. Naively, one might expect that since we are interested in states that maintain all the microscopic symmetries, the mean-field Ansatz should be invariant under their operation (e.g., lattice translations). While this is a sufficient condition for invariance, it is not a necessary one, due to the presence of the local $U(1)$ transformations described above. A symmetry operation might return the Ansatz to a $U(1)$ transformed form, which would suffice, since the same spin wave function will be obtained on projection. Hence, symmetry transformations that leave the Ansatz invariant in general will contain the naive transformation combined with a local $U(1)$ transformation. The set of all transformations that leave a mean ansatz invariant is called the projective symmetry group (PSG).⁹ In principle, we would like to associate each and every element of this group with a physical symmetry. This is because if the mean-field Ansatz is to be a faithful representation of the microscopic physics, it should have exactly as much symmetry as the original model. However, we always find that there are some elements of the PSG that are pure local transformation of the kind (11). The set of such elements also forms a group (a subgroup of the PSG) and is called the invariant gauge group (IGG). These cannot be the result of a physical symmetry. It is therefore natural to associate these elements with the emergent gauge group that describes the spin-liquid phase obtained (if the mean-field state survives projection). Therefore the first step is to identify the IGG of a mean-field Ansatz.

The invariant gauge group for Schwinger boson mean-field theories. A general Schwinger boson mean-field Hamiltonian with explicit global $SU(2)$ symmetry (global spin-

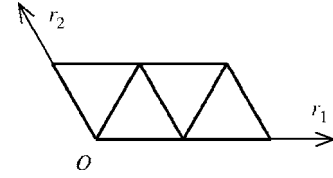


FIG. 1. Oblique coordinates system of triangular lattice.

rotation symmetry) must be of the form of Eq. (7).

It is clear that if A_{ij} and B_{ij} are both nonzero the IGG must be a Z_2 group. The only two elements of IGG are identity operation $\mathbf{1}$ and the IGG generator $-\mathbf{1}$: $b_{\mathbf{r}\sigma} \rightarrow -b_{\mathbf{r}\sigma}$. This can be seen by considering only one bond.

Note that if B_{ij} are nonzero while all A_{ij} vanish, the IGG will be a $U(1)$ group: $b_{\mathbf{r}\sigma} \rightarrow e^{i\phi} b_{\mathbf{r}\sigma}$, where ϕ is a site-independent constant. However, it is unlikely for this Ansatz to describe an antiferromagnet according to Eq. (10). Finally, we should consider the case with only nonvanishing A_{ij} . On a frustrated lattice the IGG will still be the above Z_2 group. However, if the lattice is bipartite, the IGG will be a $U(1)$ group: $b_{\mathbf{r}\sigma} \rightarrow e^{\pm i\phi} b_{\mathbf{r}\sigma}$, where we apply opposite signs on the two sublattices. This is the case of simple square lattice.

We will only consider PSGs with Z_2 IGG in the following discussion. Hence we are implicitly restricting ourselves to Z_2 spin-liquid states, which are the natural spin-liquid states on frustrated lattices within the Schwinger boson formalism.

A. Algebraic constraints on the PSG

We consider mean-field Hamiltonian that preserves all of the physical symmetries in the PSG sense (symmetric spin-liquid states). They are spin-rotation symmetry, lattice space-group symmetries, and time-reversal symmetry. The spin-rotation symmetry is already implemented by considering mean-field ansatz of the form (7), which is explicitly invariant under global $SU(2)$ spin rotations. We will consider time-reversal symmetry at the end of our derivation. The operations that we will now pay special attention to are the space-group symmetries (translations and point-group operations for the triangular lattice). As discussed before, these can be implemented via combining the naive transformation with a local (gauge) $U(1)$ transformation. One can ask the question—is it possible to have mean-field ansatz with any choice of the gauge transformations? It turns out that there are algebraic relations among the symmetry-group elements that strongly constrain the possible choices of gauge transformations. Thus, to obtain all possible PSGs we should first check the algebraic structure of PSGs without reference to a specific mean-field ansatz. The possible PSGs allowed by the algebra of the space group are defined as the algebraic PSGs related to the space group.

For the isotropic triangular lattice, the space group is generated by two translations T_1 and T_2 , one reflection σ in a bond, and the 60° rotation $R_{\pi/3}$ about a lattice site.

We use the following oblique coordinate system. In this system a site index \mathbf{r} has two integer components $\mathbf{r}=(r_1, r_2)$ (Fig. 1).

Then the four generators are given by the following formulas:

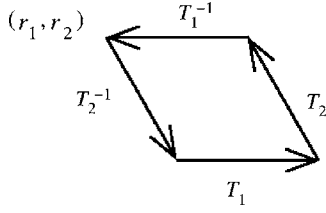


FIG. 2. An example of a relation between space-group elements $T_1^{-1}T_2T_1T_2^{-1}=\mathcal{I}$, that leads to an algebraic constraint on the PSG.

$$T_1: (r_1, r_2) \rightarrow (r_1 + 1, r_2), \quad (13a)$$

$$T_2: (r_1, r_2) \rightarrow (r_1, r_2 + 1), \quad (13b)$$

$$\sigma: (r_1, r_2) \rightarrow (r_2, r_1), \quad (13c)$$

$$R_{\pi/3}: (r_1, r_2) \rightarrow (r_1 - r_2, r_1). \quad (13d)$$

For symmetric spin-liquid states there must be four gauge-group transformations G_{T_1} , G_{T_2} , G_σ , and $G_{R_{\pi/3}}$, such that the mean-field Ansatz is invariant under $G_{T_1}T_1$, $G_{T_2}T_2$, $G_\sigma\sigma$, and $G_{R_{\pi/3}}R_{\pi/3}$, respectively. We can represent the four gauge operations by their phase,

$$G_X: b_{\mathbf{r}\sigma} \rightarrow e^{i\phi_X(\mathbf{r})} b_{\mathbf{r}\sigma}, \quad (14)$$

where the X are T_1 , T_2 , σ , and $R_{\pi/3}$, respectively.

The PSG is generated by combining the generators of the IGG: -1 , and the above four compound operators $G_X X$.

The structure of the space group imposes algebraic constraints on the G_X . For instance, the combination of translations shown in Fig. 2 should be equivalent to the identity, i.e., $T_1^{-1}T_2T_1T_2^{-1}=\mathcal{I}$. Therefore we require that the implementation of these symmetries in the PSG $[(G_{T_1}T_1)^{-1}G_{T_2}T_2G_{T_1}T_1(G_{T_2}T_2)^{-1}]$ must be the equivalent of an identity operation, which means it is an element of the IGG, either 1 or -1 . This string can be rewritten as $T_1^{-1}G_{T_1}^{-1}T_1T_1^{-1}G_{T_2}T_1(T_1^{-1}T_2)G_{T_1}(T_1^{-1}T_2)^{-1}(G_{T_2})^{-1}$. Using the fact that for a space-group operation Y , the gauge transformation $(Y)^{-1}G_X Y$ acting on site \mathbf{r} will just give a phase $\phi_X[Y(\mathbf{r})]$ (where $Y(r)$ is the image of r under the space-group operation Y), we end up with the equation

$$-\phi_{T_1}[T_1(\mathbf{r})] + \phi_{T_2}[T_1(\mathbf{r})] + \phi_{T_1}[T_2^{-1}T_1(\mathbf{r})] - \phi_{T_2}(\mathbf{r}) = p_1\pi, \quad (15)$$

where $p_1 \in \{0, 1\}$ is independent of the site index \mathbf{r} , and arises from the fact that the identity operation can be any one of the two elements of the IGG.

This kind of algebraic constraints strictly restrict the possible structures of PSG. It turns out (the proof is in Appendix A) that there is only a finite set of such constraints, which if satisfied guarantees that all relations between space-group elements are satisfied. These relations, beginning with the one described above, are

$$T_2T_1 = T_1T_2, \quad (16a)$$

$$T_1R_{\pi/3} = R_{\pi/3}T_2^{-1}, \quad (16b)$$

$$T_2R_{\pi/3} = R_{\pi/3}T_1T_2, \quad (16c)$$

$$T_1\sigma = \sigma T_2, \quad (16d)$$

$$T_1\sigma = \sigma T_2, \quad (16e)$$

$$R_{\pi/3}^{-1} = [R_{\pi/3}]^5, \quad (16f)$$

$$\sigma^{-1} = \sigma, \quad (16g)$$

$$R_{\pi/3}\sigma = \sigma[R_{\pi/3}]^5. \quad (16h)$$

These relations place severe constraints on the allowed PSGs. The most general solution that satisfies them is

$$\phi_{T_1}(r_1, r_2) = 0, \quad (17a)$$

$$\phi_{T_2}(r_1, r_2) = p_1\pi r_1, \quad (17b)$$

$$\phi_\sigma(r_1, r_2) = p_2\pi/2 + p_1\pi r_1 r_2, \quad (17c)$$

$$2\phi_{R_{\pi/3}}(r_1, r_2) = p_3\pi + p_1\pi r_2(r_2 - 1 + 2r_1), \quad (17d)$$

where p_1, p_2, p_3 are either 0 or 1. Thus there are at most eight distinct Schwinger boson symmetric spin-liquid states on isotropic triangular lattice. If we put more conditions on the mean-field ansatz (e.g., that the nearest-neighbor A_{ij} are nonzero), then the number of possible symmetric spin-liquid states is reduced from eight.

A detailed derivation of the above formulas is given in Appendix A. Also, we include the solution of algebraic PSGs on the anisotropic triangular lattice.

B. From PSGs to mean field Hamiltonians: Nearest-neighbor models

If we assume that nearest-neighbor amplitudes A_{ij} are nonzero (which is natural given that nearest-neighbor interactions in physical models tend to be dominant and usually antiferromagnetic), there are more constraints on the possible PSG structures.

This can be seen as follows. Since σ maps bond $(0,0) \rightarrow (1,1)$ to itself, we must have $\phi_\sigma(0,0) + \phi_\sigma(1,1) = 0 \pmod{2\pi}$. This imposes the constraint $p_2 = p_1 \pmod{2}$. Also, bonds $(0,0) \rightarrow (-1,0)$ and $(0,0) \rightarrow (1,0)$ are related by a 180° rotation, $(R_{\pi/3})^3$, and by antisymmetry and translation T_1 we have $A_{(0,0) \rightarrow (-1,0)} = -A_{(-1,0) \rightarrow (0,0)} = -A_{(0,0) \rightarrow (1,0)}$. This leads to another constraint,

$$\begin{aligned} \phi_{R_{\pi/3}}(-1,0) + \phi_{R_{\pi/3}}(0,1) + \phi_{R_{\pi/3}}(1,1) + 3\phi_{R_{\pi/3}}(0,0) \\ = \pi \pmod{2\pi}, \end{aligned}$$

which fixes $p_3 = 1 - p_1 \pmod{2}$.

Thus we have only two nonequivalent PSGs, corresponding to $p_1 = 0$, which we call the zero-flux state or $p_1 = 1$, which we call the π -flux state.

1. Zero-flux state

This state is specified in terms of the integers $p_1 = 0$, $p_2 = 0$, $p_3 = 1$, or equivalently, in terms of the phase factors

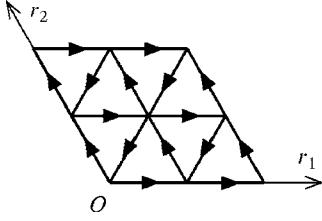


FIG. 3. Ansatz of the zero-flux state. An arrow from site i to site j means $A_{ij} > 0$. All A_{ij} have the same magnitude. All B_{ij} are real and of uniform magnitude (not shown).

involved in implementing the space-group operations,

$$\phi_{T_1}(r_1, r_2) = \phi_{T_2}(r_1, r_2) = \phi_{\sigma}(r_1, r_2) = 0,$$

$$\phi_{R_{\pi/3}}(r_1, r_2) = \pi/2.$$

We can now ask what mean-field Ansatz would be characterized by such a PSG. The mean-field Ansatz is specified by the amplitudes A_{ij} and B_{ij} on the various bonds. For this PSG, B_{ij} and A_{ij} on nearest neighbor are both real and non-zero in general. Explicit expressions for this Ansatz are

$$A_{(r_1, r_2) \rightarrow (r_1+1, r_2)} = A_{(r_1, r_2) \rightarrow (r_1, r_2+1)} = -A_{(r_1, r_2) \rightarrow (r_1+1, r_2+1)} = A_1,$$

$$B_{(r_1, r_2) \rightarrow (r_1+1, r_2)} = B_{(r_1, r_2) \rightarrow (r_1, r_2+1)} = B_{(r_1, r_2) \rightarrow (r_1+1, r_2+1)} = B_1.$$

The PSG predicts that next-nearest-neighbor A must be zero. Since $A_{ij} = -A_{ji}$ is real and antisymmetric, it is natural to represent it by oriented bonds. Figure 3 is a pictorial representation of the ansatz for the zero-flux state.

This ansatz has explicit translational invariance and has been studied by Sachdev using the large- N method.¹⁵

2. π -flux state

This state is specified in terms of the integers $p_1=1$, $p_2=1$, $p_3=0$, or equivalently, in terms of the phase factors involved in implementing the space-group operations,

$$\phi_{T_1}(r_1, r_2) = 0,$$

$$\phi_{T_2}(r_1, r_2) = \pi r_1,$$

$$\phi_{\sigma}(r_1, r_2) = (\pi/2) + \pi r_1 r_2,$$

$$\phi_{R_{\pi/3}}(r_1, r_2) = \pi r_1 r_2 + (\pi/2) r_2 (r_2 - 1).$$

The mean-field ansatz that realizes this PSG is as follows. While the nearest-neighbor bond A_{ij} is real and nonzero, the nearest-neighbor bond B_{ij} must be zero. Expressions of the Ansatz are

$$\begin{aligned} (-1)^{r_2} A_{(r_1, r_2) \rightarrow (r_1+1, r_2)} &= -A_{(r_1, r_2) \rightarrow (r_1, r_2+1)} \\ &= -(-1)^{r_2} A_{(r_1, r_2) \rightarrow (r_1+1, r_2+1)} \\ &= A_1, \end{aligned}$$

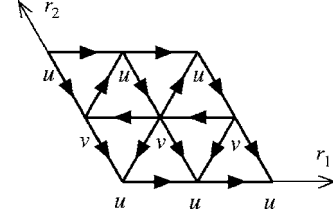


FIG. 4. Ansatz of the π -flux state. All nearest-neighbor A_{ij} are real and of the same magnitude and are positive in the directions shown. All nearest-neighbor B_{ij} are zero. The unit cell for the Schwinger bosons is doubled due to the flux, and u and v are the two sites in this unit cell.

$$B_{(r_1, r_2) \rightarrow (r_1+1, r_2)} = B_{(r_1, r_2) \rightarrow (r_1, r_2+1)} = B_{(r_1, r_2) \rightarrow (r_1+1, r_2+1)} = 0.$$

The PSG also predicts that the next-nearest-neighbor B must be zero. Note, for this state the translation symmetry is not explicit in the mean-field Hamiltonian, hence the unit cell for the Schwinger bosons is doubled. This π -flux Ansatz for the nearest-neighbor model is shown in Fig. 4.

These two states can also be distinguished by the gauge-invariant phase of the product $A_{ij}(-A_{jk}^*)A_{kl}(-A_{li}^*)$, where i, j, k, l form a rhombus with unit-length sides. This quantity was introduced by Tchernyshyov *et al.*²³ as the flux in the rhombus in bosonic large- N theory. Defining

$$|A_1|^4 e^{i\Phi} = A_{ij}(-A_{jk}^*)A_{kl}(-A_{li}^*), \quad (18)$$

where $|A_1|$ is the uniform magnitude of A_{ij} , we have that for the zero-flux state, the flux $\Phi=0$ for all rhombi, while for the π -flux state $\Phi=\pi$ for all rhombi. Therefore these two states are clearly not gauge-equivalent mean-field states.

Finally, we can consider time-reversal symmetry \hat{T} . Because the two ansatz are both real, they directly respect T symmetry, since time-reversal transformation will change the Ansatz to their complex conjugate. It is then an interesting question to ask what kind of PSG can support \hat{T} -breaking Ansatz. It turns out that one must also break lattice-reflection symmetry to obtain a time-reversal breaking state. In Appendix B we list the solutions of algebraic PSGs for anisotropic triangular lattice and the realizations in the nearest-neighbor model, which do support a \hat{T} -breaking Ansatz.

IV. ANALYSIS OF THE MEAN-FIELD THEORIES

We now study the mean-field theories arising from the Ansatz described previously. Given the PSG classification, it follows that these different mean-field solutions will be local minima of the mean-field energy. In order to pick which of these is favored with a particular Hamiltonian, one needs to compare energies between these states, which is left to the next section. Here we content ourselves with describing the properties of each of these mean-field Ansätze. The discussion closely parallels Sachdev's large- N solution of triangular lattice and Kagomé lattice.¹⁵ We also take the quantum parameter κ as a continuous number, although for Schwinger bosons derived from $SU(2)$ spins of size S , $\kappa=2S$. For small κ , the spinon dispersion will be gapped and we have a spin-

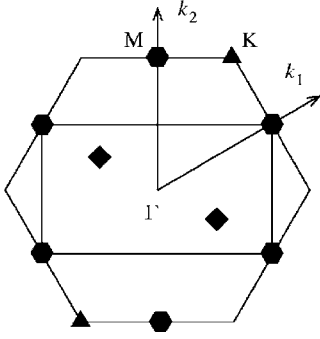


FIG. 5. Triangular lattice Brillouin zone (BZ) and k -space coordinate system. The large hexagon is the BZ of the original lattice and the zero-flux ansatz. The large rectangle is the BZ of the π -flux ansatz. Black triangles at K -points: $\pm(2\pi/3, 2\pi/3)$ are the minima of the spinon dispersion of the zero-flux state, and are also the wave vectors of magnetic ordering of the zero-flux state (120° state). Black diamonds at $\pm(\pi/2, -\pi/2)$ are the minima of the spinon dispersion of the π -flux state. Black hexagons at M -points: $\pm(\pi, -\pi)$, $\pm(-\pi, 0)$, $\pm(\pi, 0)$ are the magnetic-ordering wave vectors of the π -flux state.

liquid mean-field ground state. When κ goes beyond certain critical value κ_c , spinon dispersion becomes gapless, bosonic spinons condense, and magnetic long-range order develops. For simplicity we present only the solution to the nearest-neighbor model.

A. Zero-flux state

The mean-field theory of this state is almost identical to Sachdev's large- N theory for triangular lattice¹⁵ and the phases obtained are continuously connected to the phases described in that work. The only difference is that we include the parameter B_{ij} , which is not present in the large- N treatment, and therefore our spinon dispersion and critical quantum parameter κ_c differ slightly. This is reviewed briefly here before turning to a similar analysis of the π -flux state.

The Brillouin zone for the triangular lattice and our choice of coordinate systems in \mathbf{k} -space is shown in Fig. 5. In this oblique coordinates system, $\mathbf{k} \cdot \mathbf{r} = k_1 r_1 + k_2 r_2$. For convenience we define $k_3 = -k_1 - k_2$.

After Fourier transformation, the nearest-neighbor mean-field Hamiltonian (7) is

$$H_{MF} = \sum_{\mathbf{k}} \Psi(\mathbf{k})^\dagger D(\mathbf{k}) \Psi(\mathbf{k}) + N_s [\mu + \mu\kappa - 3J_1(B_1^2 - A_1^2)],$$

where N_s is the number of sites and the vector spinon field $\Psi(\mathbf{k})$ and the two-by-two matrix $D(\mathbf{k})$ are

$$\Psi(\mathbf{k}) = \begin{pmatrix} b_{\mathbf{k}\uparrow} \\ b_{-\mathbf{k}\downarrow}^\dagger \end{pmatrix}, \quad (19)$$

$$D(\mathbf{k}) = \begin{pmatrix} J_1 B_1 \operatorname{Re}(\xi_{\mathbf{k}}) - \mu & -iJ_1 A_1 \operatorname{Im}(\xi_{\mathbf{k}}) \\ iJ_1 A_1 \operatorname{Im}(\xi_{\mathbf{k}}) & J_1 B_1 \operatorname{Re}(\xi_{\mathbf{k}}) - \mu \end{pmatrix}, \quad (20)$$

where $\xi_{\mathbf{k}} = e^{ik_1} + e^{ik_2} + e^{-i(k_1+k_2)}$.

After a Bogoliubov transformation

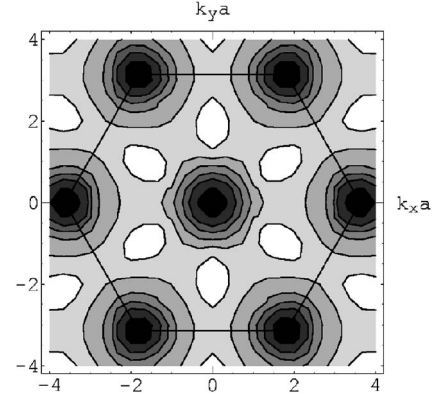


FIG. 6. The lower edge of the two-spinon spectrum for the zero-flux state at $\kappa=0.3$. Axes are in dimensionless units $k_{x,y}a$ where a is the lattice constant. The darker regions have lower energy. The 120° magnetic order arises from magnon condensation at the zone corners (see also Fig. 5).

$$\begin{pmatrix} b_{\mathbf{k}\uparrow} \\ b_{-\mathbf{k}\downarrow}^\dagger \end{pmatrix} = M_{\mathbf{k}} \begin{pmatrix} \gamma_{\mathbf{k}\uparrow} \\ \gamma_{-\mathbf{k}\downarrow}^\dagger \end{pmatrix}, \quad (21)$$

where $M_{\mathbf{k}} \in SU(1, 1)$ is chosen to diagonalize the mean-field Hamiltonian,

$$H_{MF} = \sum_{\mathbf{k}} \omega(\mathbf{k}) (\gamma_{\mathbf{k}\uparrow}^\dagger \gamma_{\mathbf{k}\uparrow} + \gamma_{-\mathbf{k}\downarrow}^\dagger \gamma_{-\mathbf{k}\downarrow} + 1) + N_s [\mu + \mu\kappa - 3J_1(B_1^2 - A_1^2)],$$

where the spinon dispersion $\omega(\mathbf{k})$ is

$$\omega(\mathbf{k}) = \sqrt{[J_1 B_1 \operatorname{Re}(\xi_{\mathbf{k}}) - \mu]^2 - [J_1 A_1 \operatorname{Im}(\xi_{\mathbf{k}})]^2} \quad (22)$$

and the self-consistency equations are

$$6J_1 A_1 = - \int_{BZ} \frac{\partial \omega(\mathbf{k})}{\partial A_1} \mathbf{d}^2 k, \quad (23)$$

$$6J_1 B_1 = + \int_{BZ} \frac{\partial \omega(\mathbf{k})}{\partial B_1} \mathbf{d}^2 k, \quad (24)$$

$$1 + \kappa = - \int_{BZ} \frac{\partial \omega(\mathbf{k})}{\partial \mu} \mathbf{d}^2 k, \quad (25)$$

where the integral is over the Brillouin zone, and the integration measure $\mathbf{d}^2 k = dk_1 dk_2 / (4\pi^2)$.

The mean-field energy per bond is

$$E/\text{bond} = J_1(B_1^2 - A_1^2). \quad (26)$$

Minima of the spinon dispersion are at $(k_1, k_2) = \pm(2\pi/3, 2\pi/3)$, which are the corners of the Brillouin zone. The two-spinon spectrum also has minima at the Brillouin zone corners and at the zone center. As in Ref. 11, we display in Fig. 6 a contour plot of the minimum energy required to create a two-spinon excitation at a given crystal momentum (the lower edge of the two-spinon spectrum) to show this feature.

By solving $\min \omega(\mathbf{k})=0$ together with self-consistent equations, we determined the critical quantum parameter $\kappa_c \approx 0.42$. We can estimate the sublattice magnetization for the spin-1/2 Heisenberg model to be 58% of classical spin, which probably overestimates the order since it is larger than that obtained from spin-wave theories, which predicts this to be about 48%.²⁴

B. π -flux state

From Fig. 4, it is clear that there are two sites in a unit cell, distinguished by the parity of r_2 . We label them by u and v .

After Fourier transformation, the mean-field Hamiltonian (7) is

$$H_{MF} = \sum_{\mathbf{k}} \Psi(\mathbf{k})^\dagger D(\mathbf{k}) \Psi(\mathbf{k}) + N_s [\mu + \mu\kappa + 3J_1 A_1^2]. \quad (27)$$

Here $\sum_{\mathbf{k}}$ sums over $(N_s/2)$ \mathbf{k} points in the spinon Brillouin zone, which is one half of the hexagonal Brillouin zone of original spin model (see Fig. 5).

The vector spinon field $\Psi(\mathbf{k})$ is

$$\Psi(\mathbf{k}) = \begin{pmatrix} b_{u\mathbf{k}\uparrow} \\ b_{v\mathbf{k}\uparrow} \\ b_{u-\mathbf{k}\downarrow}^\dagger \\ b_{v-\mathbf{k}\downarrow}^\dagger \end{pmatrix} \quad (28)$$

and the four-by-four matrix $D(\mathbf{k})$ has the following block form:

$$\begin{pmatrix} \mu \cdot \mathbf{1} & -iP(\mathbf{k}) \\ iP(\mathbf{k})^\dagger & \mu \cdot \mathbf{1} \end{pmatrix}, \quad (29)$$

where $\mathbf{1}$ is the two-by-two identity matrix, and the two-by-two Hermitian matrix $P(\mathbf{k})$ can be written in terms of the Pauli matrices $\sigma^{x,y,z}$,

$$P(\mathbf{k}) = J_1 A_1 [\sin(k_1)\sigma^z - \sin(k_2)\sigma^x - \cos(k_3)\sigma^y]. \quad (30)$$

This Hamiltonian can be diagonalized by a Bogoliubov transformation using a $SU(2,2)$ matrix after which we have

$$H_{MF} = \sum_{\mathbf{k}; a=u,v} \omega(\mathbf{k}) (\gamma_{a\mathbf{k}\uparrow}^\dagger \gamma_{a\mathbf{k}\uparrow} + \gamma_{a-\mathbf{k}\downarrow}^\dagger \gamma_{a-\mathbf{k}\downarrow} + 1) + N_s [\mu + \mu\kappa + 3J_1 A_1^2], \quad (31)$$

where γ are transformed boson operators and $a=u,v$ is a sublattice index.

The spinon dispersion is therefore fourfold degenerate with the form

$$\omega(\mathbf{k}) = \sqrt{\mu^2 - J_1^2 A_1^2 [\sin^2(k_1) + \sin^2(k_2) + \cos^2(k_3)]}.$$

Self-consistent equations come from the minimization of mean-field energy (constant terms after Bogoliubov transformation),

$$6J_1 A_1 = - \int_{BZ} \frac{\partial \omega(\mathbf{k})}{\partial A_1} \mathbf{d}^2 k, \quad (32)$$

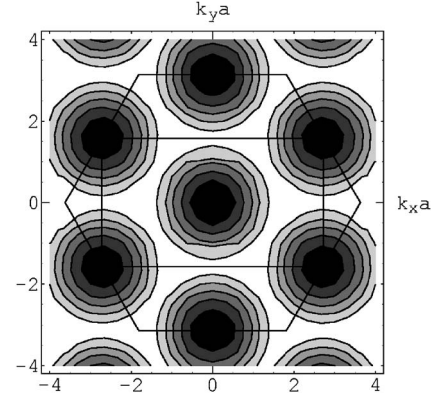


FIG. 7. The lower edge of the two-spinon spectrum of the π -flux state with $\kappa=0.3$. Axes are in dimensionless units $k_{x,y}a$ where a is the lattice constant. The darker regions have lower energy. Magnetic order arises from magnon condensation at the centers of the zone edges (see also Fig. 5).

$$1 + \kappa = - \int_{BZ} \frac{\partial \omega(\mathbf{k})}{\partial \mu} \mathbf{d}^2 k, \quad (33)$$

where the integral is over the Brillouin zone, and $\mathbf{d}^2 k = dk_1 dk_2 / (4\pi^2)$. Recall that the amplitudes B_{ij} on nearest-neighbor bonds are forbidden in this state by the PSG.

On solving the self-consistent equations, the mean-field energy per bond is obtained as

$$E/\text{bond} = -J_1 A_1^2, \quad (34)$$

and the minima of spinon dispersion are at $(k_1, k_2) = \pm(\pi/2, -\pi/2)$. Therefore the minima of the two-spinon spectrum are at the Brillouin zone edge centers and center, as illustrated in Fig. 7. The distinction from the analogous diagram for the zero-flux state in Fig. 6 indicates that the π -flux state is really a distinct state from the zero-flux state.

The critical quantum parameter for the π -flux state is found to be $\kappa_c \approx 0.75$. This large κ_c makes the π -flux state a promising candidate of spin liquid, especially given that in the zero-flux case the mean-field theory seemed to overestimate magnetic order. Even in the event that magnetic order is present, it is expected to be weak, and the presence of a proximate spin liquid should be apparent at finite temperatures and energies as discussed in Ref. 16. However, for the nearest-neighbor antiferromagnet, the zero-flux state always has lower mean-field energy, which is consistent with the general argument of flux expulsion by Tchernyshyov *et al.*²³ Later we will see that the π -flux state can be stabilized as the global minimum of the mean-field theory, if other terms such as next-neighbor couplings or ring exchange are present in the Hamiltonian.

C. Spin configurations from spinon condensates

When quantum parameter κ goes beyond its critical value the spinon dispersion becomes zero at several \mathbf{k} points. Bosons condense at those \mathbf{k} points, namely, the spinon field $\Psi(\mathbf{k})$ receives an expectation value in ground state. We briefly analyze the structure of condensates and the corre-

sponding spin configurations for the zero-flux state, where we follow Ref. 15, and then apply the same analysis to the π -flux state on the triangular lattice.

The zero-flux state has spinon minima at $\mathbf{k}_c = (2\pi/3, 2\pi/3)$. At this point, $D(\mathbf{k}_c)$ of Eq. (20) has an eigenvector with zero eigenvalue

$$\Psi_1 = (i, 1)^T$$

(T is transposition). When κ just exceeds κ_c , a condensate at \mathbf{k}_c is obtained; $\langle \Psi(\mathbf{k}_c) \rangle = (\langle b_{\mathbf{k}_c \uparrow} \rangle \langle b_{-\mathbf{k}_c \downarrow}^\dagger \rangle) = c_1 \Psi_1$. Similarly, $D(-\mathbf{k}_c)$ has one eigenvector associated with zero eigenvalue

$$\Psi_2 = (-i, 1)^T = \Psi_1^*.$$

A condensate at $-\mathbf{k}_c$ is $\langle \Psi(-\mathbf{k}_c) \rangle = c_2 \Psi_2$. Here $c_{1,2}$ are two complex numbers.

The condensate on lattice site \mathbf{r} is then given by

$$x \equiv \begin{pmatrix} \langle b_{\mathbf{r} \uparrow} \rangle \\ \langle b_{\mathbf{r} \downarrow} \rangle \end{pmatrix} = \begin{pmatrix} ic_1 & -ic_2 \\ c_2^* & c_1^* \end{pmatrix} \begin{pmatrix} e^{i\mathbf{k}_c \cdot \mathbf{r}} \\ e^{-i\mathbf{k}_c \cdot \mathbf{r}} \end{pmatrix}$$

and the ordered magnetic moment is $\mathbf{S}(\mathbf{r}) = (1/2)x^\dagger \sigma x$.

This can be readily shown to give rise to the 120° classical Néel state in which the classical spin is

$$\mathbf{S}(\mathbf{r}) = \mathbf{n}_1 \cos(\mathbf{Q} \cdot \mathbf{r}) + \mathbf{n}_2 \sin(\mathbf{Q} \cdot \mathbf{r}), \quad (35)$$

where $\mathbf{n}_{1,2}$ are orthogonal to each other and have the same length as the classical spin

$$\mathbf{n}_1^2 = \mathbf{n}_2^2 = \mathbf{S}^2. \quad (36)$$

$\mathbf{Q} = \pm(2\pi/3, 2\pi/3)$ is the wave vector of the Brillouin zone corner, represented as small triangles in Fig. 5.

For the π -flux state, the critical spinon wave vector occurs at $\mathbf{k}_c = (\pi/2, -\pi/2)$. At this point, $D(\mathbf{k}_c)$ of Eq. (29) has two eigenvectors associated with zero eigenvalue,

$$\Psi_1 = \left(\frac{1-i}{\sqrt{3}}, -\frac{i}{\sqrt{3}}, 0, 1 \right)^T,$$

$$\Psi_2 = \left(\frac{i}{\sqrt{3}}, -\frac{1+i}{\sqrt{3}}, 1, 0 \right)^T,$$

The condensate at \mathbf{k}_c can in general be parametrized as $\langle \Psi(\mathbf{k}_c) \rangle = c_1 \Psi_1 + c_2 \Psi_2$. Similarly, $D(-\mathbf{k}_c)$ has two eigenvectors associated with zero eigenvalue,

$$\Psi_3 = \left(\frac{1+i}{\sqrt{3}}, \frac{i}{\sqrt{3}}, 0, 1 \right)^T = \Psi_1^*,$$

$$\Psi_4 = \left(-\frac{i}{\sqrt{3}}, -\frac{1-i}{\sqrt{3}}, 1, 0 \right)^T = \Psi_2^*,$$

and the condensate at $-\mathbf{k}_c$ is parametrized as $\langle \Psi(-\mathbf{k}_c) \rangle = c_3 \Psi_3 + c_4 \Psi_4$. Here $c_{1,2,3,4}$ are four complex numbers.

Returning to real space, the spinon condensate on sublattice u is

$$x_u \equiv \begin{pmatrix} \langle b_{u\mathbf{r} \uparrow} \rangle \\ \langle b_{u\mathbf{r} \downarrow} \rangle \end{pmatrix} = \begin{pmatrix} \frac{1-i}{\sqrt{3}}c_1 + \frac{i}{\sqrt{3}}c_2 & \frac{1+i}{\sqrt{3}}c_3 - \frac{i}{\sqrt{3}}c_4 \\ c_4^* & c_2^* \end{pmatrix} \begin{pmatrix} e^{i\mathbf{k}_c \cdot \mathbf{r}} \\ e^{-i\mathbf{k}_c \cdot \mathbf{r}} \end{pmatrix},$$

while the spinon condensate on sublattice v is

$$x_v \equiv \begin{pmatrix} \langle b_{v\mathbf{r} \uparrow} \rangle \\ \langle b_{v\mathbf{r} \downarrow} \rangle \end{pmatrix} = \begin{pmatrix} -\frac{i}{\sqrt{3}}c_1 - \frac{1+i}{\sqrt{3}}c_2 & \frac{i}{\sqrt{3}}c_3 - \frac{1-i}{\sqrt{3}}c_4 \\ c_3^* & c_1^* \end{pmatrix} \begin{pmatrix} e^{i\mathbf{k}_c \cdot \mathbf{r}} \\ e^{-i\mathbf{k}_c \cdot \mathbf{r}} \end{pmatrix}.$$

The ordered magnetic moment on sublattice p is $(1/2)(x_p)^\dagger \sigma x_p$ for $p=u,v$, respectively, and is present at wave vectors at the midpoints of the Brillouin zone edges shown via black hexagons in Fig. 5.

Under the constraint that the magnitude of condensate is uniform (which is required to have uniform magnitude for the ordered moments), we find a continuum of four-sublattices ordered states, which is consistent with previous classical energy analysis on triangular lattice magnets with interactions that favor order at these wave vectors.²⁵ The classical spin in the four-sublattices states is

$$\mathbf{S}(\mathbf{r}) = \mathbf{n}_1(-1)^{r_1} + \mathbf{n}_2(-1)^{r_2} + \mathbf{n}_3(-1)^{r_1+r_2}, \quad (37)$$

where $\mathbf{n}_{1,2,3}$ are three vectors orthogonal to each other, and

$$\mathbf{n}_1^2 + \mathbf{n}_2^2 + \mathbf{n}_3^2 = \mathbf{S}^2. \quad (38)$$

Generally speaking, this configuration is noncoplanar if $|\mathbf{n}_{1,2,3}|$ are all nonzero. However, a previous analysis confirmed the existence of ‘‘order from disorder’’ phenomena, namely, quantum or thermal fluctuation will lift the accidental degeneracy and favor a collinear state in large S models with next-nearest-neighbor antiferromagnetic exchange,^{26,27} which corresponds to the case that only one of $\mathbf{n}_{1,2,3}$ is non-zero.

It has been argued that ring exchange will favor a noncoplanar state.²⁵ The classical ground state will then be a tetrahedral configuration with an equal angle between any two of the four spins. In the above expression, this state is realized when $\mathbf{n}_{1,2,3}$ have the same magnitude.

However, on studying the ordered state with weak spinon condensation, the constraint that the magnitude of the spinon condensate is uniform enforces the additional condition on the $\mathbf{n}_{1,2,3}$ that one of the following three equations must be satisfied:

$$|\mathbf{n}_1| = |\mathbf{n}_2| + |\mathbf{n}_3|, \quad (39a)$$

$$\text{or } |\mathbf{n}_2| = |\mathbf{n}_3| + |\mathbf{n}_1|, \quad (39b)$$

$$\text{or } |\mathbf{n}_3| = |\mathbf{n}_1| + |\mathbf{n}_2|. \quad (39c)$$

Thus the classical degeneracy is not entirely lifted at this level. Also, neither the collinear state nor the tetrahedral state can be obtained from weak spinon condensates from this

spin-liquid state—although the wave vectors of all these ordered states are identical. This implies that if there is a continuous phase transition out of the π -flux spin-liquid phase, the proximate spin-ordered state is not the collinear or tetrahedral state, but these are realized via further phase transitions on increasing the size of the spin. We are still seeking a simple explanation for these results.

V. HAMILTONIANS STABILIZING THE π -FLUX STATE

The π -flux spin-liquid state differs in several respects from the zero-flux state; also, its stability against magnetic ordering up to a relatively large quantum parameter $\kappa_c=0.75$ (in a nearest-neighbor model) suggests its physics may be important for understanding physical spin-1/2 models. Hence it is of interest to ask what interactions might stabilize such a π -flux state.

A clue is provided by the fact that the lowest-energy triplet excitations of such a state are located at the midpoints of the Brillouin zone edges. This is precisely the ordering wave-vector for classical spins on the triangular lattice in a model with next-nearest-neighbor (J_2) antiferromagnetic interactions in addition to nearest-neighbor antiferromagnetic interactions (J_1) in the range $0.125J_1 < J_2 < J_1$.²⁶ It is conceivable that on reducing the size of the spin in this model from infinity (the classical limit) to $S=1/2$, the system enters a spin-liquid state described by the π -flux state, although strictly the quantum parameter for this case is $\kappa=1$.

A second possibility arises from ring exchange—it is well known that there are several realizations of $S=1/2$ quantum antiferromagnets on the triangular lattice where ring exchange plays an important role. These include monolayers of ³He adsorbed on graphite,³ and the organic quantum antiferromagnet κ -(ET)₂ Cu₂(CN)₃.² Also, exact diagonalization studies of the triangular lattice $S=1/2$ magnet with ring exchange has uncovered unusual properties.⁵ In a recent variational study with fermionic mean-field states by Motrunich¹⁷ it was found that ring exchange of the sign that arises naturally with electrons, favors a state with zero flux. Here we will investigate the effect of ring exchange on the Schwinger boson states—in particular, for which sign of the exchange one might favor the π -flux state. We find that including four-spin ring exchange with the sign as obtained from the Hubbard model stabilizes the π -flux state.

Here we give some physical arguments as to why next-neighbor antiferromagnetic interactions and the ring term will stabilize the π -flux state over the zero-flux state.

A. Effect of next-neighbor interactions J_2

For the zero-flux state, nearest-neighbor amplitudes B_1 and A_1 , and next-nearest-neighbor amplitudes B_2 are nonzero, while the next-nearest-neighbor amplitude A_2 is zero. Note that B_2 is nonzero even if next-nearest-neighbor coupling J_2 is zero.

$$\frac{E^{[\text{zero-flux}]}}{\text{bond } J_1} = (B_1^{[\text{zero-flux}]})^2 - (A_1^{[\text{zero-flux}]})^2 + \frac{J_2}{J_1} (B_2^{[\text{zero-flux}]})^2.$$

In contrast, for the π -flux state, A_1 and A_2 are nonzero, while B_1 and B_2 are zero. Note, A_2 is nonzero even if J_2 is zero.

$$\frac{E^{[\pi\text{-flux}]}}{\text{bond } J_1} = - (A_1^{[\pi\text{-flux}]})^2 - \frac{J_2}{J_1} (A_2^{[\pi\text{-flux}]})^2.$$

It is readily shown with the self-consistent values of the mean-field amplitudes that for $J_2=0$, $E^{[\text{zero-flux}]} < E^{[\pi\text{-flux}]}$, i.e., the zero-flux state is preferred at the mean-field level. However, if we increase J_2 from zero, we do not expect the Ansatz to change rapidly, thus the energy for the zero-flux state will have a positive slope with respect to J_2 , while the π -flux state has a negative slope. We may then expect a first-order transition between the two states. This is consistent with the previous analysis of the J_1 - J_2 model in the opposite limit of semiclassical spins, where a transition between the 120° state (the magnetically ordered analog of the zero-flux state) and the collinear state (the magnetically ordered analog of the π -flux state) is found on increasing J_2 .^{27,28} From the classical energy analysis,²⁶ we know that in large S limit $\alpha=1/8$ is the critical point between different ordered states with ordering wave vectors at the BZ corners vs. BZ edge midpoints. Thus one might expect that a moderate next-nearest-neighbor term ($1/8 < \alpha < 1$) will stabilize the π -flux state over the zero-flux state in the quantum limit, since these states have short-range order (two spinon minima) at precisely these wave vectors. We now provide estimates for the phase boundary (the critical ratio $\alpha=J_2/J_1$) between the zero-flux and π -flux spin-liquid phases as a function of the quantum parameter κ .

Small κ analysis. The competition between different spin-liquid states can be studied analytically in the limit of small κ .²³ In this case the magnitude of the Ansatz A_{ij} and B_{ij} are small. Then, we can develop a series expansion of the self-consistent equations in κ , and find solutions.

First, we use this expansion to look at the J_1 - J_2 model, with $\alpha \equiv J_2/J_1 < 1$ and sufficiently small quantum parameter κ .

The energy difference between the zero-flux and the π -flux state in this limit is

$$\begin{aligned} \frac{E^{[\text{zero-flux}]} - E^{[\pi\text{-flux}]}}{\text{bond } J_1} = & - (1 - \alpha) \left[\frac{\kappa}{6} \right]^2 + \frac{2\alpha}{1 - \alpha} \left[\frac{\kappa}{6} \right]^3 \\ & + \left(\frac{87}{4} + 23\alpha + 72\alpha^2 \right) \left[\frac{\kappa}{6} \right]^3 + O(\kappa^4). \end{aligned} \quad (40)$$

From the above expressions for mean-field energy difference, we can find the transition point between the zero-flux and π -flux states to lowest order in κ ;

$$\alpha_c = 1 - \sqrt{\kappa/3}. \quad (41)$$

In the limit of vanishing κ the zero-flux state is preferred until the next-neighbor bond is stronger than the nearest-neighbor bond. However, this critical ratio decreases rapidly with increasing κ .

In the small- κ limit one can ignore the spin-carrying excitations. Then, going beyond the mean-field theory the rel-

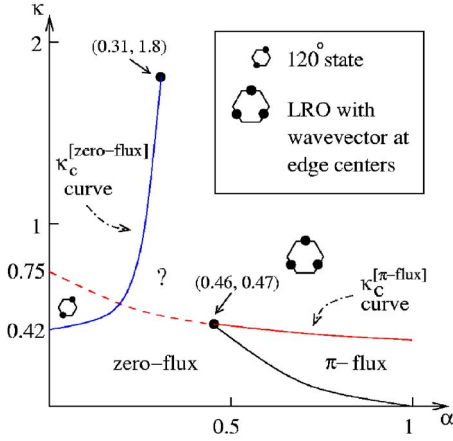


FIG. 8. (Color online) The mean-field phase diagram of the triangular lattice antiferromagnet with nearest-neighbor J_1 and next-neighbor J_2 interactions, as a function of the ratio $\alpha = J_2/J_1$ and quantum parameter κ . The diagram is a quantitatively reliable solution of mean-field equations in the region near to and below the red line (dashed and solid) where spinon condensation of the π -flux state occurs. Just above the solid red line, magnetic ordering at the Brillouin zone M point occurs, while below it the π -flux spin-liquid phase is obtained. The black line is the first-order phase boundary between the zero-flux and π -flux spin-liquid phases, while the blue line represents the onset of 120° magnetic order. The quick rise of this line to large values of κ is due to the frustration of the 120° Néel order by next-neighbor interactions. If uninterrupted by magnetic order (of the M type) this may open a window of spin liquid for physical spin values in this model.

evant degrees of freedom are the gauge excitations, which in this case correspond to those of an Ising gauge theory. The distinction between zero- and π -flux states in this limit we believe has to do with the sign of the plaquette energy term that penalizes Ising vortex excitations in the case of the zero-flux state, but prefers a ground state with a uniform background “flux” of such vortices in the case of the π -flux state.

Numerical solution. The mean-field equations can be numerically solved to obtain the competition between the zero-flux and π -flux states and states with magnetic order. This is shown in Fig. 8. The critical value $\kappa_c^{[\pi\text{-flux}]}$ at which spinon condensation occurs for the π -flux state is shown by the dashed and solid red line. If the π -flux state is stabilized, then above this line spinon condensation leads to magnetic order at the BZ edge centers (M points). There are a number of distinct ordering patterns consistent with this ordering wave vector—which makes an analysis of the ordered phase a delicate one; and we do not attempt it here. Therefore, the phase diagram shown in Fig. 8 is strictly speaking only to be trusted below this $\kappa_c^{[\pi\text{-flux}]}$ line (red line). However, certain extrapolations above this line can be made with some degree of confidence.

The first-order phase boundary between the π -flux and the zero-flux spin-liquid states is shown by the black line in Fig. 8. At small κ it approaches $\alpha=1$ via the analytic form derived previously [Eq. (41)]. It intersects the spinon condensation line for the π -flux state at $\alpha=0.46$, $\kappa=0.47$.

The zero-flux state is stabilized at smaller values of α , and sufficiently small quantum parameter $\kappa < \kappa_c^{[\text{zero-flux}]}$, where

the critical quantum parameter for spinon condensation in this state is shown by the blue line. Spinon condensation is expected to lead to the 120° state on crossing this line.²⁹ Again, this is most reliably established if the ordered states with wave vectors at the M points (M states) are not in the picture, which is the case below the dashed red line in Fig. 8. An interesting aspect of the phase diagram is the large values of $\kappa_c^{[\text{zero-flux}]} \approx 1.8$ that arise if the M states are neglected. This is believed to be a result of frustration of the 120° Néel order by next-neighbor interactions. While some part of this spin-liquid region in the phase diagram above $\kappa_c^{[\pi\text{-flux}]}$ might be occupied eventually by magnetically ordered M states, the existence of zero-flux spin-liquid states for fairly large values of the quantum parameter is likely to persist, making the J_1 - J_2 model an interesting candidate for spin-liquid physics that deserves further attention.

B. Effect of ring exchange

In addition to the exchange interaction between a pair of spins, multispin interactions are also present in insulators with nonnegligible charge fluctuations. While for spin one-half systems, the three-spin interaction can be expressed in terms of two-spin exchange, a new term is generated when considering four-spin interactions. The four-spin ring-exchange term is

$$H_{\text{Ring}} = J_{\text{Ring}} \sum (P_4 + \text{H.c.}), \quad (42)$$

$$P_4 = b_{i\delta}^\dagger b_{i\alpha} b_{j\alpha}^\dagger b_{j\beta} b_{k\beta}^\dagger b_{k\gamma} b_{l\gamma}^\dagger b_{l\delta}, \quad (43)$$

where P_4 is the four-spin permutation operator, which is written out conveniently in terms of the Schwinger boson operators as above. The sites i, j, k, l form a rhombus and $\alpha, \beta, \gamma, \delta \in \{\uparrow, \downarrow\}$ are spin indices. The above bosonic spinon representation of the ring exchange may be checked by expanding it in terms of the spin operators in the spin-1/2 case and verifying it has the required form.³⁰ A more efficient way to prove this identity will be to establish a correspondence with the fermionic spinon representation of ring exchange, which is done later in this section.

From the t/U expansion of the Hubbard model,³¹ it is found that $J_{\text{Ring}} = 20t^4/U^3$ and is positive. In the following, when we consider the ring-exchange term we neglect the next-nearest-neighbor term, and vice versa. Evaluating the ring-exchange term in the mean-field ground state, one finds that the result contains

$$\langle H_{\text{Ring}} \rangle_{\text{MF}} = 8J_{\text{Ring}} (A_{ij} A_{jk}^* A_{kl} A_{li}^* + \text{c.c.}) + \dots, \quad (44)$$

which is the term we used to define flux. The other terms are small, especially in the small- κ regime. This term clearly has different signs for zero-flux and π -flux states, and favors the π -flux states when J_{Ring} is positive. Thus we also expect a possible transition from a zero-flux state to a π -flux state when we tune ring-exchange coupling.

It is well known that the ring-exchange term, derived from the Hubbard model, has a positive (negative) coupling constant when expressed in terms of a permutation operator, if the loop length is even (odd).³² This can be seen as fol-

lows. Since the ring-exchange term arises from a virtual electron hopping process lowering the energy, the effective term generated is $-K_L[c_{1\sigma_L}^\dagger c_{L\sigma_L} c_{L\sigma_{L-1}}^\dagger c_{L-1\sigma_{L-1}} \cdots c_{2\sigma_1}^\dagger c_{1\sigma_1} + \text{H.c.}]$, where $c_{i\sigma}$ are electron annihilation operators with site index i and spin index σ , and $K_L > 0$. Clearly, this term includes a permutation operator for length L loop $(-1)^{L-1}(-K_L)c_{1\sigma_L}^\dagger c_{1\sigma_1} c_{2\sigma_1}^\dagger c_{2\sigma_2} \cdots c_{L\sigma_{L-1}}^\dagger c_{L\sigma_L} + \text{H.c.}$ So for L even we have $+K_L(P_L + \text{H.c.})$.

While the above discussion has been phrased in terms of fermionic spinons, we can now translate those observations into the bosonic spinon language. It turns out that the permutation operator has the same form and sign in terms of both fermion (electron) operators and Schwinger boson operators. We give two arguments in support of this below. First, notice that spin-1/2 operators have the same representation in a Schwinger boson and a ‘‘Schwinger fermion’’ (electrons) scheme. Assume that spin indices α, β take values of $+1$ (spin up) and -1 (spin down). For the $S=1/2$ system we have $c_{i\alpha}^\dagger c_{i\beta} = (2S + 2\alpha S^z) \delta_{\alpha,\beta} + [(1+\alpha)S^+ + (1-\alpha)S^-] \delta_{\alpha,-\beta} = b_{i\alpha}^\dagger b_{i\beta}$. Therefore we can simply replace fermion operator c by Schwinger boson operator b in the permutation operator. The second argument is to use the Jordan-Wigner transformation to change electronic operators into boson. After replacing fermionic operators with bosons the Jordan-Wigner string operators become a constant under the constraint of constant $(2S)$ particles on each site.

Now we evaluate the above ring-exchange operator for longer-length loops in the Schwinger boson mean-field states. We focus on even-length loops since we expect the dominant amplitudes to be given by the A_{ij} s, which can only give rise to even-length loops if they are the only amplitudes that count. The dominant term is $2 \cdot 2^{L/2} (A_{1,2} A_{2,3}^* \cdots A_{L-1,L} A_{L,1}^* + \text{H.c.})$. This is not exactly the term-defining flux in the loop,²³ which has an additional minus sign for each A^* . Namely, the result is $2 \cdot 2^{L/2} / (-1)^{L/2}$ (term-defining flux + H.c.). It is then clear that for $L=4, 8, 12, \dots$ the ring-exchange term favors π flux in the loop, while for $L=6, 10, 14, \dots$ it favors zero flux. It is amusing to contrast this with the result for mean-field theories based on a fermionic spin representation, where ring exchange favors states with zero flux.¹⁷ The difference has to do with the different definitions for flux that naturally appear in these two theories.

Small- κ analysis. As argued previously, raising the value of J_{Ring}/J_1 above a critical value, favors the π -flux state over the zero-flux state. We now study the effect of the ring-exchange term by evaluating it in the zero-flux and π -flux states, in the limit of small κ where an analytic solution may be obtained. Another benefit for going to small- κ limit is that larger-ring exchange effect (e.g., length-6 ring) is controlled by small parameter κ as $\kappa^{\text{length}/2}$ according to Tchernyshov *et al.*,²³ therefore only the energetics of the ring, namely, the rhombus, is important.

The procedure described above is of course only the lowest-order term, but we expect it to give us the correct qualitative behavior. For zero-flux state, the contribution from the ring-exchange term is $(\kappa^2/6)J_{\text{Ring}}$ per rhombus to lowest order. For the π -flux state, it is $-(\kappa^2/18)J_{\text{Ring}}$ per rhombus to lowest order. Therefore, a positive J_{Ring} clearly

TABLE I. Approximate finite- κ result for critical J_{Ring}/J_1 at which the zero-flux state gives way to the π -flux state on the triangular lattice.

κ	J_{Ring}/J_1
0.05	0.126
0.10	0.127
0.20	0.128
0.30	0.129

favors the π -flux state. Since for every site, there are three bonds and three rhombi on average, we can find the transition point in the $\kappa \rightarrow 0$ limit to be

$$[J_{\text{Ring}}/J_1]_c = 1/8. \quad (45)$$

Several other theories predict a transition for the triangular lattice antiferromagnet while tuning this ratio J_{Ring}/J_1 , although the phases appearing may be different. Motrunich’s fermionic variational method¹⁷ predicts a transition from a ‘‘ π -flux’’ fermionic mean-field state to a ‘‘zero-flux’’ mean-field state when J_{Ring}/J_1 increases over about 0.35. A previous bosonic mean-field phase diagram²⁰ predicts a transition from a 120° Néel-ordered state to a collinear-ordered state when this ratio increases over $1/3$. It is interesting that we found a similar transition between two disordered spin-liquid states for sufficiently small κ , with short-ranged order at precisely these two wave vectors, as this ratio is increased.

Numerical solution. For finite κ , the numerical solution of the mean-field equations has been obtained for the nearest-neighbor model below the critical value κ_c for both states. We can make a lowest order perturbative treatment of the next-nearest-neighbor and ring-exchange terms, namely, we evaluate these two terms in the mean-field ground state of the nearest-neighbor model and thus obtain the transition point. We found the approximate critical value of $\alpha \equiv J_2/J_1$ and J_{Ring}/J_1 , listed in Table I.

VI. SPIN-LIQUID STATES ON THE KAGOMÉ LATTICE

The Kagomé lattice has three sites in one unit cell, labeled by u, v, w (see Fig. 9).

We label a unit cell by $\mathbf{r} = (r_1, r_2)$ and label a site by $(r_1, r_2)_p$ where $p = u, v, w$.

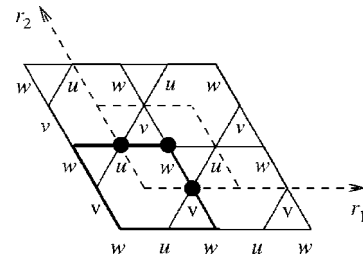


FIG. 9. Coordinates system of Kagomé lattice. Rhombus enclosed by dashed lines is the unit cell at origin. Three sites with black dots form the basis of the lattice. Black rhombus is an example of length-8 loops.

A. PSG analysis of the Kagomé lattice

We would like to obtain the possible symmetric spin-liquid states on the Kagomé lattice described within the Schwinger boson approach. Again, a PSG analysis will be carried out just as was done on the triangular lattice. A gauge transformation G is then described by three phase functions $\phi_u(\mathbf{r}), \phi_v(\mathbf{r}), \phi_w(\mathbf{r})$.

For simplicity we will consider Ansätze with $A_{ij} = \frac{1}{2} \epsilon_{\sigma\sigma'} \langle b_{i\sigma} b_{j\sigma'} \rangle$ only. These amplitudes are naturally present for predominantly antiferromagnetic interactions, and can be strictly justified in the large- N limit.¹⁵ Then, due to the frustrated nature of the Kagomé lattice, the IGG is Z_2 , generated by

$$\phi_u(\mathbf{r}) = \phi_v(\mathbf{r}) = \phi_w(\mathbf{r}) = \pi,$$

thus we will study Z_2 spin-liquid states within the Schwinger boson approach.

In the above coordinates system the space group is generated by two translations T_1, T_2 , reflection σ , and 60° rotation $R_{\pi/3}$. The first two generators preserve sublattices. The reflection exchanges u and v sublattices. The rotation is a cyclic permutation of three sublattices $u \rightarrow v, v \rightarrow w, w \rightarrow u$.

For each space-group generator X we can associate a gauge transformation described by three phase functions $\phi_{X,u}(\mathbf{r}), \phi_{X,v}(\mathbf{r}), \phi_{X,w}(\mathbf{r})$.

The procedure of solving for the different PSGs allowed by the algebraic constraints imposed by relations between symmetry elements is parallel to the triangular case, except that one has to keep track of the index of sublattices. It turns out that the three phase functions can be chosen to be identical. The solution of the algebraic PSG (details in Appendix C) is then identical to the triangular lattice case except that the phase functions have one more index.

$$\phi_{T_1,p}(r_1, r_2) = 0, \quad (46a)$$

$$\phi_{T_2,p}(r_1, r_2) = p_1 \pi r_1, \quad (46b)$$

$$\phi_{\sigma,p}(r_1, r_2) = p_2 \pi/2 + p_1 \pi r_1 r_2, \quad (46c)$$

$$2\phi_{R_{\pi/3},p}(r_1, r_2) = p_3 \pi + p_1 \pi r_2 (r_2 - 1 + 2r_1), \quad (46d)$$

where $p=u, v, w$. Thus, in the case of the Kagomé lattice too, there are not more than eight symmetric Z_2 spin-liquid states, corresponding to the two values that each of the p_1, p_2, p_3 can take on.

If we now specialize to states that have nonvanishing nearest-neighbor amplitudes A_{ij} , we have more realizations of the algebraic PSG. The only additional restriction (cf. Sec. III B) is that bond $(0,0)_u \rightarrow (0,0)_w$ can be related to bond $(0,0)_v \rightarrow (0,0)_w$ by both reflection and 60° rotation. This gives one constraint $p_2 = 1 - p_3$. In all these Ansätze the amplitudes A_{ij} are real and of uniform magnitude.

B. Spin-liquid states on the Kagomé

The four realizations are listed below. We will use the same convention of the \mathbf{k} -space coordinates system as the

triangular case by taking the lattice constant as unity (the length of the nearest-neighbor bond is $1/2$). It is convenient to divide the four states into two pairs, two with $p_1=0$ and two with $p_1=1$. The first condition implies that the generators of translation commute, the analog of the zero-flux state, while the second condition implies a flux of π in a unit cell. It will turn out that the two zero-flux states correspond to the two states discussed earlier by Sachdev in the context of the Kagomé lattice, while the two π -flux states have not previously been discussed.

The zero-flux states. (1) The first state we consider is characterized by $p_1=0, p_2=0, p_3=1$. This is the large- N ground state identified by Sachdev for the nearest-neighbor antiferromagnet, which he called $Q_1 = -Q_2$ state.¹⁵

This state has zero flux in both the length-6 hexagon and the length-8 rhombus, hence we will also refer to it as [0Hex, 0Rhom]. Its critical quantum parameter $\kappa_c \approx 0.54$. The spinon dispersion has minima at the corners of Brillouin zone $\mathbf{k} = \pm(2\pi/3, 2\pi/3)$, and so does the two-spinon spectrum. After spinon condensation it gives rise to the $\sqrt{3} \times \sqrt{3}$ magnetically ordered classical ground state.

(2) The second state we consider is characterized by $p_1=0, p_2=1, p_3=0$. This is another state considered by Sachdev and was called the $Q_1 = Q_2$ state.¹⁵

This state has π flux in the length-6 hexagon and zero flux in the length-8 rhombus, hence we will also refer to it as [π Hex, 0Rhom]. Its critical quantum parameter $\kappa_c \approx 0.50$. The spinon dispersion has minima at the centers of Brillouin zone $\mathbf{k} = (0, 0)$; so does the two-spinon spectrum. After spinon condensation it gives rise to the translational invariant classical ground state.

The π -flux states. (3) The third state we consider is characterized by $p_1=1, p_2=0, p_3=1$. The ansatz is given in Fig. 19 in Appendix C and has not been considered before. Due to the presence of flux in the unit cell, a doubled the unit cell needs to be considered for the spinons.

This state has π flux in both the length-6 hexagon and the length-8 rhombus, hence we will also refer to it as [π Hex, π Rhom]. Thus, in a nearest-neighbor model it is expected to have the highest energy of the four states for the same κ in the small- κ regime.

Its critical quantum parameter is fairly large, $\kappa_c \approx 0.93$. The minima of spinon dispersion is at $\mathbf{k} = \pm(\pi/6 + n\pi, \pi/6 + m\pi)$, where n, m are integers (see Fig. 10). Thus the two-spinons spectrum lower edge has minima at $\pm(\pi/3 + n\pi, \pi/3 + m\pi)$ and $(n\pi, m\pi)$. In addition to the Brillouin zone center, corners, and edge centers, minima are also present at the halfway points to the corners.

(4) The last state we consider is $p_1=1, p_2=1, p_3=0$. The ansatz is given in Fig. 11 and has not been considered before.

This state has zero flux in the length-6 hexagon and π flux in the length-8 rhombus, hence we will also refer to it as [0Hex, π Rhom]. It is potentially the most interesting of the states considered so far since its critical quantum parameter $\kappa_c \approx 2.0$ is greater than unity. This means that this state is very likely to be a symmetric spin-liquid state for the spin-1/2 system if it can be realized. The large value of κ_c is a result of the dispersion of the relevant spinon bands being nearly flat along certain directions in the Brillouin zone.

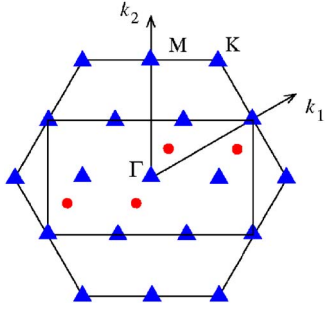


FIG. 10. (Color online). \mathbf{k} space of the Kagomé lattice. The large hexagon is the Brillouin zone of the original Kagomé lattice and the two $p_1=0$ Ansätze. The large rectangle is the Brillouin zone of the two $p_1=1$ Ansätze, which enclose a flux of π in their unit cells. The red dots are the minima of the spinon dispersion for both $p_1=1$ states within the reduced Brillouin zone. The blue triangles are the locations of the minima of the lower edge of the two-spinon spectrum for both $p_1=1$ states.

However, since this state has π flux in the length-8 rhombus, it is, by the general argument of flux expulsion by Tchernyshyov *et al.*²³ expected to have a higher mean-field energy than Sachdev's ground state if we consider a pure nearest-neighbor Heisenberg model. In the small κ limit the energy difference will be the order of κ^4 . However, it must also be kept in mind that mean-field energetics is not precisely the same as the true energetics of the system.

Given the interesting nature of this state we can ask what interactions are likely to stabilize it within mean-field theory, relative to the Sachdev ground state. From our previous analysis of ring exchange we know that adding ring-exchange interactions of the sign obtained from the Hubbard model favors zero flux in loops of length six and π flux in loops of length eight. This is precisely satisfied by loops in this Ansatz as can be checked from Fig. 11. Therefore the Kagomé antiferromagnet with ring exchange may be a good system to realize a spin-liquid phase.

The position of minima of the spinon dispersion and of the two-spinons spectrum lower edge are the same as in the previous state: $p_1=1, p_2=0, p_3=1$. However, the spinon dis-

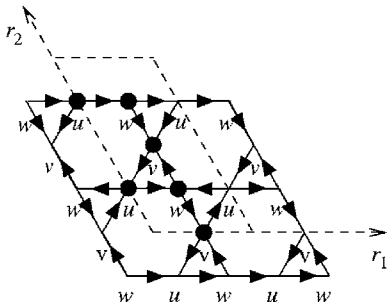


FIG. 11. Ansatz of the $p_1=1, p_2=1, p_3=0$ state. The presence of π flux in the Kagomé lattice unit-cell leads to unit cell doubling, which is now defined by the dashed rhombus. Six sites with black dots form the basis. All nearest-neighbor A_{ij} are real and of the same magnitude, and are positive in the directions shown. This spin-liquid Ansatz has zero flux in the length-6 hexagonal loops but π flux in the length-8 loops such as the rhombus, hence [0Hex, π Rhom]. It has a large critical quantum parameter $\kappa_c=2.0$.

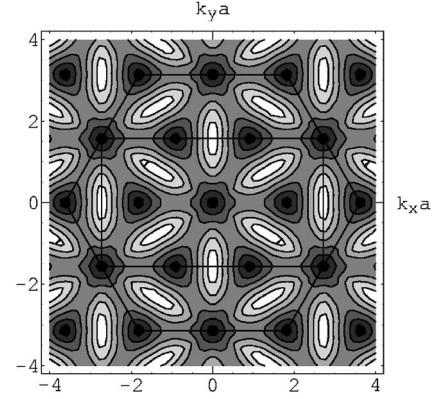


FIG. 12. Two-spinons spectrum lower edge of the $p_1=1, p_2=1, p_3=0$ state at $\kappa=\kappa_c=2.0$. Axes are in dimensionless unit $k_{x,y}a$ where a is lattice constant (two times nearest-neighbor distance). Darker regions have lower energy. Although the two-spinon minima occur at the same wave-vector locations as in the previous $p_1=1, p_2=0, p_3=1$ state, the differences in the dispersion are apparent.

persions of these two states are not identical. In particular, the present $p_1=1, p_2=1, p_3=0$ state has three doubly degenerate dispersion branches while as previously discussed the $p_1=1, p_2=0, p_3=1$ state has six nondegenerate dispersion branches. Other differences between these two states may be observed in the contour plots of the lower edge of the two-spinon dispersions in Fig. 12 and 13, respectively. A variety of magnetically ordered states can arise from spinon condensation in both these cases; the magnetic states so obtained and the associated quantum transitions would be an interesting topic for future study.

VII. CONCLUSIONS

We have extended the projective symmetry-group analysis, previously used to classify fermionic mean-field states, to bosonic mean-field states of quantum antiferromagnets on the triangular and Kagomé lattices. This allowed us to access fundamentally different spin-liquid states and ensure that po-

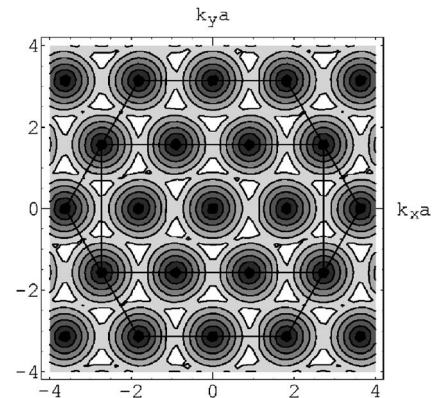


FIG. 13. Two-spinons spectrum lower edge of the $p_1=1, p_2=0, p_3=1$ state at $\kappa=\kappa_c=0.9$. Axes are in dimensionless unit $k_{x,y}a$ where a is the lattice constant (two times nearest-neighbor distance). The darker regions have lower energy.

tentially interesting states were not overlooked. On the triangular lattice a new Z_2 symmetric spin-liquid state (π -flux state) emerged from this analysis and was studied. This state is distinct from the previously studied bosonic mean-field state (zero flux or Sachdev state), which can be seen in that they have different spinon and two-spinons dispersions. The nature of the ordered state resulting from spinon condensation turns out to be more intricate in this case, as is the quantum-ordering transition, and is a topic for further study. Although this state is less favorable from the point of view of mean-field energy as compared to the zero-flux state in the case of nearest-neighbor interactions, it is stabilized by the inclusion of moderate next-nearest-neighbor or ring-exchange interactions with signs as derived from the Hubbard model. The mean-field analysis suggests that the triangular lattice model with next-neighbor antiferromagnetic interactions might be favorable for realizing spin-liquid ground states.

We have also studied Z_2 symmetric spin-liquid states on the Kagomé lattice using the PSG technique. Again we find only a few candidate states, in particular, two physically interesting states are found, which are analogous to the π -flux state on the triangular lattice. In particular, one of these states has a remarkably large value for the critical quantum parameter $\kappa_c=2.0$, which implies that if realized, it would be stable against magnetic order for physical values of the spin. We find that ring-exchange interactions would stabilize precisely this state, making the Kagomé model with ring exchange an attractive model to study in the search for spin-liquid phases. The stability of these states to other forms of order, such as valence bond solid order, is important to understand but were not addressed in the present work. Also, the relation between fermionic mean-field states, classified via the $SU(2)$ PSGs and the bosonic spinon mean-field theories studied in this paper with their $U(1)$ PSGs remains unclear and is a topic for future study.

ACKNOWLEDGMENTS

We would like to thank O. Motrunich and C. Nayak for discussions. A.V. was supported by A. P. Sloan Foundation and by DOE LDRD DEA 3664LV.

APPENDIX A: SOLUTION TO ALGEBRAIC PSGS OF TRIANGULAR LATTICE

In this appendix we derive the allowed PSGs for symmetric spin liquids on the triangular lattice characterized by a Z_2 gauge group. Essentially, we need to make sure that the constraints imposed by various identities between symmetry-group elements are satisfied by the PSG. In particular, the ansatz must satisfy the relations in Eqs. (16a)–(16h). It turns out that if a PSG satisfies all these constraints, then other relations between symmetry-group elements are automatically satisfied. This is because any group element written as a string containing products of generators can be brought into a “normal ordered” form using just these operations where normal ordering implies a form of the kind $\sigma^s [R_{\pi/3}]^r T_1^{t_1} T_2^{t_2}$ where $s \in \{0, 1\}$, $r \in \{0, 1, \dots, 5\}$ and t_1, t_2

$\in \mathcal{Z}$. This is sufficient to show no new constraints are imposed by other relations between symmetry operations.

To simplify expressions we introduce forward difference operators Δ_1 and Δ_2 , defined as $\Delta_1 f(r_1, r_2) \equiv f(r_1+1, r_2) - f(r_1, r_2)$ and $\Delta_2 f(r_1, r_2) \equiv f(r_1, r_2+1) - f(r_1, r_2)$.

We should first consider how PSG changes if we do a gauge transformation G to the ansatz. After the gauge transformation, the ansatz will be invariant under $GG_X XG^{-1} = GG_X XG^{-1} X^{-1} X$. Therefore, G_X should be replaced by $GG_X XG^{-1} X^{-1}$. In terms of phases,

$$\phi_X(\mathbf{r}) \rightarrow \phi_G(\mathbf{r}) + \phi_X(\mathbf{r}) - \phi_G[X^{-1}(\mathbf{r})]. \quad (\text{A1})$$

As in Wen’s derivation of fermionic PSG, we make the following assumption: using gauge freedom, we can make the Ansatz explicitly invariant under translation T_1 , or, $\phi_{T_1}(\mathbf{r})=0$. For triangular lattice, this can be done by solving equations $\phi_G(r_1, r_2) + \phi_{T_1}(r_1, r_2) - \phi_G(r_1-1, r_2)=0$. Since ϕ_X is a phase, unless explicitly mentioned, all equations of phases in this section are true modulo 2π .

Then we add the generator T_2 . Since $T_1^{-1} T_2 T_1 T_2^{-1} = \mathcal{I}$, following the procedure in the example in the main text, we have the equation,

$$\Delta_1 \phi_{T_2}(r_1, r_2) = p_1 \pi,$$

where p_1 is a site-independent integer. Due to the 2π periodicity, p_1 has only two distinct choices: 0 and 1, and $-p_1 \equiv p_1 \pmod{2}$. Other integer parameters, p_n and p'_n , in this section also have this property.

The solution of ϕ_{T_2} is then

$$\phi_{T_2}(r_1, r_2) = \phi_{T_2}(0, r_2) + p_1 \pi r_1.$$

Here we make another assumption: using the gauge freedom, we can further make $\phi_{T_2}(0, r_2)=0$, while preserving $\phi_{T_1}(\mathbf{r})=0$. Then the solution simplifies to

$$\phi_{T_2}(r_1, r_2) = p_1 \pi r_1. \quad (\text{A2})$$

In the above, we made two assumptions, $\phi_{T_1}(\mathbf{r})=0$ and $\phi_{T_2}(0, r_2)=0$. These two equations can be satisfied if we have open boundary condition. However, great care must be taken for periodic boundary condition before we proceed. In this section we always assume open boundary condition, and the two assumptions can be realized by exploiting gauge freedom.

After this gauge-fixing procedure we are still left with three gauge freedoms. The first one is adding a global constant phase,

$$G_1: \phi_1(\mathbf{r}) = \text{const}. \quad (\text{A3})$$

According to Eq. (A1) this will not change any generator of PSG. We can use this freedom to fix one of A_{ij} to be real positive.

The second gauge freedom is

$$G_2: \phi_2(r_1, r_2) = \pi r_1. \quad (\text{A4})$$

At first sight ϕ_{T_1} will be changed under this gauge transformation. According to Eq. (A1), after applying G_2 ,

$$\phi_{T_1}(r_1, r_2) \rightarrow \phi_2(r_1, r_2) + \phi_{T_1}(r_1, r_2) - \phi_2(r_1 - 1, r_2) \rightarrow \pi.$$

However, we are free to add a site-independent constant π to any $\phi_{\chi}(\mathbf{r})$ because of the IGG structure; so this gauge transformation does not really change G_{T_1} and G_{T_2} .

Similar to this one, we have the third gauge freedom,

$$G_3: \quad \phi_3(r_1, r_2) = \pi r_2. \quad (\text{A5})$$

G_2 and G_3 do not change G_{T_1} and G_{T_2} , but will certainly modify other generators of PSG. Later we will use them to eliminate redundant parameters in our solution.

We can now include generators of the point group into consideration. First consider the reflection σ .

Algebraic constraints from $T_1^{-1}\sigma T_2\sigma^{-1}=\mathcal{I}$ and $T_2^{-1}\sigma T_1\sigma^{-1}=\mathcal{I}$ are

$$\Delta_1\phi_{\sigma}(r_1, r_2) = p'_2\pi + p_1r_2\pi,$$

$$\Delta_2\phi_{\sigma}(r_1, r_2) = p'_3\pi + p_1r_1\pi.$$

The solution to these equations is

$$\phi_{\sigma}(r_1, r_2) = \phi_{\sigma}(0, 0) + p'_2r_1\pi + p'_3r_2\pi + p_1r_1r_2\pi.$$

Further constraint from $\sigma\sigma=\mathcal{I}$ is $p'_2=p'_3 \pmod 2$ and $2\phi_{\sigma}(0, 0)=p_2\pi$.

Under the gauge transformation G_2 , the solution becomes

$$\begin{aligned} \phi_{\sigma}(r_1, r_2) &\rightarrow \phi_2(r_1, r_2) + \phi_{\sigma}(r_1, r_2) - \phi_2(r_2, r_1) \\ &\rightarrow \phi_{\sigma}(0, 0) + (p'_3 + 1)(r_1 + r_2)\pi + p_1r_1r_2\pi, \end{aligned}$$

while ϕ_{T_1} and ϕ_{T_2} do not change. Therefore we can always assume that $p'_2=p'_3=0 \pmod 2$. Finally, we get the general solution (17c) in the main text.

We are still left with two gauge freedoms at this point. Both G_1 and G_2G_3 do not change G_{T_1} , G_{T_2} , and G_{σ} . Add the last generator $R_{\pi/3}$ to the system. Algebraic constraints from $T_1^{-1}R_{\pi/3}T_2^{-1}R_{\pi/3}^{-1}=\mathcal{I}$ and $T_2^{-1}R_{\pi/3}T_1R_{\pi/3}^{-1}=\mathcal{I}$ are

$$\Delta_1\phi_{R_{\pi/3}}(r_1, r_2) = p'_4\pi + p_1r_2\pi,$$

$$\Delta_2\phi_{R_{\pi/3}}(r_1, r_2) = p'_5\pi + p_1(r_1 - r_2 - 1)\pi.$$

The solution to these equations is

$$\begin{aligned} \phi_{R_{\pi/3}}(r_1, r_2) &= \phi_{R_{\pi/3}}(0, 0) + p'_4\pi r_1 + p'_5\pi r_2 + p_1r_1r_2\pi \\ &\quad + \frac{1}{2}p_1r_2(r_2 - 1)\pi. \end{aligned}$$

Constraint from $(R_{\pi/3})^6=\mathcal{I}$ is $12\phi_{R_{\pi/3}}(0, 0)=0$.

Further constraint from $R_{\pi/3}\sigma R_{\pi/3}\sigma^{-1}=\mathcal{I}$ is $p'_4=p'_5=0 \pmod 2$ and $4\phi_{R_{\pi/3}}(0, 0)=0$. Therefore we can assume that $\phi_{R_{\pi/3}}(0, 0)=p_3\pi/2$.

Under the gauge transformation G_2G_3 , the solution of $\phi_{R_{\pi/3}}$ transforms to

$$\begin{aligned} \phi_{R_{\pi/3}}(r_1, r_2) &\rightarrow \frac{p_3}{2}\pi + (p'_5 + 1)r_1\pi + p_1r_1r_2\pi \\ &\quad + \frac{1}{2}p_1r_2(r_2 - 1)\pi, \end{aligned}$$

while ϕ_{T_1} , ϕ_{T_2} , and ϕ_{σ} do not change. Therefore, we can

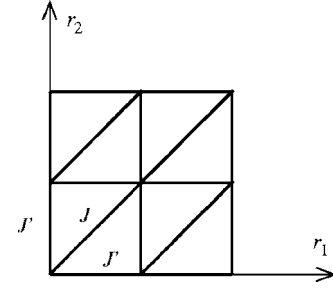


FIG. 14. Coordinates system of anisotropic triangular lattice.

always assume that $p'_5=0 \pmod 2$. Then we get the general solution (17d) in the main text.

A motivation for studying the range of states available comes from the numerical simulations⁵ on the triangular lattice $S=1/2$ model with ring exchange, where a state with a fourfold degenerate ground state and no magnetic order was found in exact diagonalization studies. While this degeneracy is consistent with a gapped Z_2 spin liquid, the quantum numbers of the degenerate states were not compatible with that expected for the simplest such spin liquid. The question then arises whether more complicated spin-liquid states could reproduce the observations. Although we answer this question in the negative for the π -flux state, the nature of a phase that could produce the observed degeneracies remains an interesting open question.

APPENDIX B: PSGs OF ANISOTROPIC TRIANGULAR LATTICE

Anisotropic triangular lattice can be realized in experimental systems such as Cs_2CuCl_4 .¹ It is also possible that the spin-liquid state breaks triangular lattice space-group symmetry down to anisotropic triangular lattice space group. A careful large- N study of the Hubbard-Heisenberg model on anisotropic triangular lattice has been carried out by Chung *et al.*³³ They used a unit cell with four sites. Our PSG analysis can actually justify their choice of unit cell within symmetric spin-liquid states. We use the following coordinates system (Fig. 14).

This space group also has four generators. The first three are identical to the isotropic case: T_1 , T_2 , and σ . The last one is replaced by a 180° rotation R_{π} .

$$R_{\pi}: \quad (r_1, r_2) \rightarrow (-r_1, -r_2). \quad (\text{B1})$$

The solution is identical to the isotropic case before solving the last generator.

For the last generator R_{π} , from constraints $T_1^{-1}R_{\pi}T_1^{-1}R_{\pi}^{-1}=\mathcal{I}$ and $T_2^{-1}R_{\pi}T_2^{-1}R_{\pi}^{-1}=\mathcal{I}$, we have two equations,

$$\Delta_1\phi_{R_{\pi}}(r_1, r_2) = p'_5\pi,$$

$$\Delta_2\phi_{R_{\pi}}(r_1, r_2) = p_4\pi.$$

The solution to these equations is

$$\phi_{R_{\pi}}(r_1, r_2) = \phi_{R_{\pi}}(0, 0) + p'_5r_1\pi + p_4r_2\pi.$$

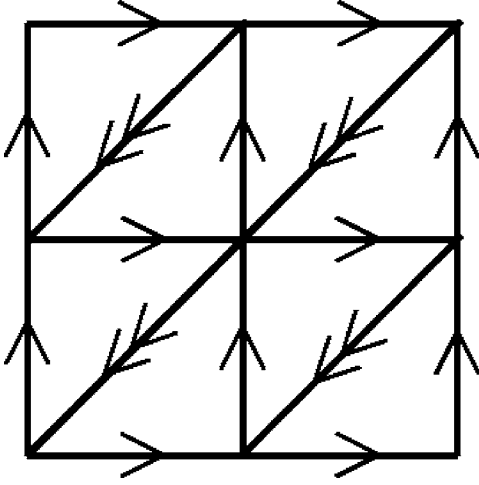


FIG. 15. Ansatz of the zero-flux state on the anisotropic triangular lattice. The different arrows represent different amplitudes of A . Single-arrow A are real. B are not represented in this picture.

The constraint from $R_\pi R_\pi = \mathcal{I}$ is $4\phi_{R_\pi}(0,0)=0$, then we can assume that $\phi_{R_\pi}(0,0)=p_3\pi/2$.

Further constraint from $\sigma R_\pi \sigma R_\pi = \mathcal{I}$ is $p'_5=p_4 \bmod 2$. However, we cannot use gauge freedom $G_2 G_3$ to eliminate p_4 this time.

The final solutions are

$$\phi_{T_1}(r_1, r_2) = 0, \quad (\text{B2a})$$

$$\phi_{T_2}(r_1, r_2) = p_1 \pi r_1, \quad (\text{B2b})$$

$$\phi_\sigma(r_1, r_2) = p_2 \pi/2 + p_1 r_1 r_2 \pi, \quad (\text{B2c})$$

$$\phi_{R_\pi}(r_1, r_2) = p_3 \pi/2 + p_4 \pi(r_1 + r_2), \quad (\text{B2d})$$

where p_1, p_2, p_3, p_4 are integers, either 0 or 1.

If nearest-neighbor A are nonzero, we have only two possible realizations. The difference from the isotropic case is, this time not all A are real. Therefore we can, in principle, have time-reversal breaking states.

Two realizations: “zero-flux state:” $p_1=0, p_2=0, p_3=1, p_4=0$.

$$\phi_{T_1}(r_1, r_2) = \phi_{T_2}(r_1, r_2) = \phi_\sigma(r_1, r_2) = 0,$$

$$\phi_{R_\pi}(r_1, r_2) = \pi/2.$$

All B are real, diagonal A can be complex, A on the other two kinds of bonds are real (see Fig. 15). “ π -flux state:” $p_1=1, p_2=1, p_3=0$, and $p_4=1$.

$$\phi_{T_1}(r_1, r_2) = 0,$$

$$\phi_{T_2}(r_1, r_2) = \pi r_1,$$

$$\phi_\sigma(r_1, r_2) = \pi/2 + r_1 r_2 \pi,$$

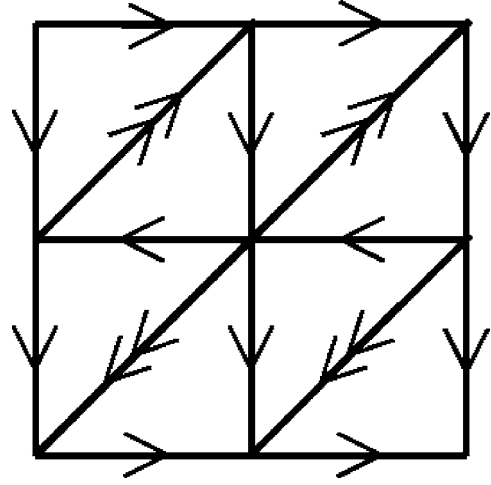


FIG. 16. Ansatz of the π -flux state on anisotropic triangular lattice. The different arrows represent different amplitudes of A . Single-arrow A are real. B are not represented in the picture.

$$\phi_{R_\pi}(r_1, r_2) = \pi(r_1 + r_2).$$

Diagonal A can be complex, diagonal B must be zero. A on the other two kinds of bonds are real, B on the other two kinds of bonds are pure imaginary (see Fig. 16).

In both states, if diagonal A are neither real nor pure imaginary, we will have nontrivial flux (not zero or π) through certain rhombi, then the ansatz breaks time-reversal symmetry. If we further impose time-reversal symmetry, diagonal A must be real in the zero-flux state, and pure imaginary in the π -flux state. However, if all B happen to be zero, diagonal A can be either real or pure imaginary in any of these two states.

The “ π -flux” symmetric spin-liquid state (with T symmetry) on anisotropic triangular lattice, has the same spinon dispersion minima positions with isotropic case, therefore they will give rise to the same magnetic-ordering wave vectors (M points: midpoints of BZ edges).

APPENDIX C: PSGS OF KAGOMÉ LATTICE

1. Properties of the different mean-field states

The zero-flux states. Ansätze for these states are shown in Figs. 17 and 18.

π -flux states. For the $p_1=1, p_2=0, p_3=1$ state, the ansatz is given in Fig. 19.

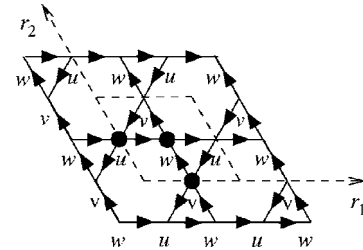


FIG. 17. Ansatz of the $p_1=0, p_2=0, p_3=1$ state, which is the $Q_1=-Q_2$ state of Sachdev, which on spinon condensation leads to the $\sqrt{3} \times \sqrt{3}$ state.

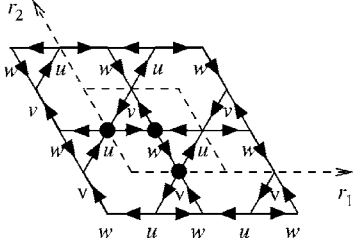


FIG. 18. Ansatz of the $p_1=0, p_2=1, p_3=0$ state, which is the $Q_1=Q_2$ state in Sachdev's notation. On spinon condensation this leads to the $q=0$ magnetically ordered state.

The mean-field Hamiltonian for these two $p_1=1$ (π -flux) states is similar to that of the π -flux state on triangular lattice, Eqs. (27) and (29). But the vector spinon field Ψ has twelve components and the $P(\mathbf{k})$ matrix becomes a six-by-six Hermitian matrix in the following form:

$$P(\mathbf{k}) = -iJ_1A_1 \begin{pmatrix} \mathcal{A}(\mathbf{k}) & \mathcal{C}(\mathbf{k}) \\ \mathcal{C}(\mathbf{k}) & \mathcal{B}(\mathbf{k}) \end{pmatrix},$$

where $\mathcal{A}(\mathbf{k})$, $\mathcal{B}(\mathbf{k})$, $\mathcal{C}(\mathbf{k})$ are three-by-three anti-Hermitian matrices.

The $\mathcal{C}(\mathbf{k})$ matrix has the same form for both $p_1=1$ states.

$$\mathcal{C}(\mathbf{k}) = \begin{pmatrix} 0 & e^{ik_3/2} & -e^{-ik_2/2} \\ -e^{-ik_3/2} & 0 & 0 \\ e^{-ik_2/2} & 0 & 0 \end{pmatrix}.$$

For the $p_1=1, p_2=1, p_3=0$ state the $\mathcal{A}(\mathbf{k})$ matrix is

$$\mathcal{A}(\mathbf{k}) = \begin{pmatrix} 0 & e^{-ik_3/2} & -e^{ik_2/2} \\ -e^{ik_3/2} & 0 & 2 \cos(k_1/2) \\ e^{-ik_2/2} & -2 \cos(k_1/2) & 0 \end{pmatrix}.$$

The $\mathcal{B}(\mathbf{k})$ matrix is

$$\mathcal{B}(\mathbf{k}) = \begin{pmatrix} 0 & -e^{-ik_3/2} & -e^{ik_2/2} \\ e^{ik_3/2} & 0 & 2i \sin(k_1/2) \\ e^{-ik_2/2} & 2i \sin(k_1/2) & 0 \end{pmatrix}.$$

For the $p_1=1, p_2=0, p_3=1$ state the $\mathcal{A}(\mathbf{k})$ matrix is

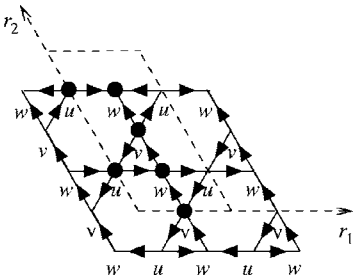


FIG. 19. Ansatz of the $p_1=1, p_2=0, p_3=1$ state. The Rhombus enclosed by dashed lines is the unit cell. Six sites with black dots form the basis.

$$\mathcal{A}(\mathbf{k}) = \begin{pmatrix} 0 & -e^{-ik_3/2} & e^{ik_2/2} \\ e^{ik_3/2} & 0 & 2i \sin(k_1/2) \\ -e^{-ik_2/2} & 2i \sin(k_1/2) & 0 \end{pmatrix}.$$

The $\mathcal{B}(\mathbf{k})$ matrix is

$$\mathcal{B}(\mathbf{k}) = \begin{pmatrix} 0 & e^{-ik_3/2} & e^{ik_2/2} \\ -e^{ik_3/2} & 0 & 2 \cos(k_1/2) \\ -e^{-ik_2/2} & -2 \cos(k_1/2) & 0 \end{pmatrix}.$$

2. Solution to the algebraic PSG on the Kagomé

The procedure for solving the algebraic PSG is described below.

The algebraic form of the four-space group generators is listed below. Note the unusual -1 in $R_{\pi/3}$. Generators T_1 and T_2 preserve sublattices.

$$T_1: (r_1, r_2)_p \rightarrow (r_1 + 1, r_2)_p,$$

$$T_2: (r_1, r_2)_p \rightarrow (r_1, r_2 + 1)_p.$$

σ exchanges u and v ,

$$\sigma: (r_1, r_2)_u \rightarrow (r_2, r_1)_v,$$

$$(r_1, r_2)_v \rightarrow (r_2, r_1)_u,$$

$$(r_1, r_2)_w \rightarrow (r_2, r_1)_w.$$

$R_{\pi/3}$ cyclicly permutes the three sublattices,

$$R_{\pi/3}: (r_1, r_2)_u \rightarrow (r_1 - r_2 - 1, r_1)_v,$$

$$(r_1, r_2)_v \rightarrow (r_1 - r_2, r_1)_w,$$

$$(r_1, r_2)_w \rightarrow (r_1 - r_2, r_1)_u.$$

As before we can assume that $\phi_{T_1,p}(\mathbf{r})=0$ and $\phi_{T_2,p}(0, r_2)=0$, for $p=u, v, w$, respectively.

From $T_1^{-1}T_2T_1T_2^{-1}=\mathcal{I}$, we have the equation

$$\Delta_1 \phi_{T_2,p}(r_1, r_2) = p_1 \pi$$

for $p=u, v, w$, respectively. Note that the constant p_1 must be the same for three sublattices.

The solution is then

$$\phi_{T_2,p}(r_1, r_2) = p_1 \pi r_1.$$

At this stage we are left with more gauge freedom than the triangular case. The first one is a uniform rotation of boson phases on all sites.

$$G_1: \phi_{1,p}(\mathbf{r}) = \text{const.}$$

As before, this gauge transformation does not change any element of PSG. We will use this freedom to fix one of A_{ij} [e.g., bond $(0,0)_u - (0,0)_w$] to be real positive.

The second and third gauge freedoms do not change G_{T_1} and G_{T_2} , but they change the other two generators. We will

use them to fix the form of G_σ . The second one has no correspondence in triangular case,

$$G_2: \quad \phi_{2,u}(\mathbf{r}) = +\phi_0,$$

$$\phi_{2,v}(\mathbf{r}) = -\phi_0,$$

$$\phi_{2,w}(\mathbf{r}) = 0,$$

where ϕ_0 is an arbitrary constant. The third one is similar to the gauge operation we used in the triangular case,

$$G_3: \quad \phi_{3,p}(r_1, r_2) = \pi r_1,$$

where $p=u, v, w$.

The fourth gauge freedom does not change G_{T_1} , G_{T_2} , and G_σ , but it changes $G_{R_{\pi/3}}$. We will use this freedom to fix the form of $G_{R_{\pi/3}}$:

$$G_4: \quad \phi_{4,u}(r_1, r_2) = \pi(r_1 + r_2),$$

$$\phi_{4,v}(r_1, r_2) = \pi(r_1 + r_2),$$

$$\phi_{4,w}(r_1, r_2) = \pi(r_1 + r_2 + 1).$$

We can now introduce the point group generator σ . Algebraic constraints from $T_1^{-1}\sigma T_2\sigma^{-1}=\mathcal{I}$ and $T_2^{-1}\sigma T_1\sigma^{-1}=\mathcal{I}$ are

$$\Delta_1\phi_{\sigma,p}(r_1, r_2) = p'_2\pi + p_1r_2\pi,$$

$$\Delta_2\phi_{\sigma,p}(r_1, r_2) = p'_3\pi + p_1r_1\pi,$$

where $p=u, v, w$, p'_2 and p'_3 are integer-constant independent of the unit-cell index (r_1, r_2) and sublattice index p . The solution to these equations is

$$\phi_{\sigma,p}(r_1, r_2) = \phi_{\sigma,p}(0, 0) + p'_2r_1\pi + p'_3r_2\pi + p_1r_1r_2\pi.$$

However, we have no a priori reason to say $\phi_{\sigma,p}(0, 0)$ are independent of sublattices index p .

Further constraint from $\sigma\sigma=\mathcal{I}$ is $p'_2=p'_3 \pmod 2$ and

$$2\phi_{\sigma,w}(0, 0) = p_2\pi,$$

$$\phi_{\sigma,u}(0, 0) + \phi_{\sigma,v}(0, 0) = p_2\pi,$$

where p_2 is an integer constant. This fixes $\phi_{\sigma,w}(0, 0)$ to be $p_2\pi/2$ but leaves one freedom for $\phi_{\sigma,u}(0, 0)$ and $\phi_{\sigma,v}(0, 0)$. As in a triangular case we can use G_3 to make $p'_2=p'_3=0$. Because after applying G_3 the solution to ϕ_σ becomes, according to Eq. (A1).

$$\phi_{\sigma,p}(r_1, r_2) \rightarrow \phi_{\sigma,p}(0, 0) + (p'_2 + 1)(r_1 + r_2)\pi + p_1r_1r_2\pi.$$

We now apply G_2 .

$$\phi_{\sigma,u}(r_1, r_2) \rightarrow \phi_{\sigma,u}(0, 0) + 2\phi_0 + p_1r_1r_2\pi,$$

$$\phi_{\sigma,v}(r_1, r_2) \rightarrow \phi_{\sigma,v}(0, 0) - 2\phi_0 + p_1r_1r_2\pi,$$

$$\phi_{\sigma,w}(r_1, r_2) \rightarrow \phi_{\sigma,w}(0, 0) + p_1r_1r_2\pi.$$

Therefore we can always make $\phi_{\sigma,u}=\phi_{\sigma,v}=p_2\pi/2$ by choosing appropriate ϕ_0 . Then the three-phase functions $\phi_{\sigma,p}$ are identical.

Add the last generator $R_{\pi/3}$ to the system. Algebraic constraints from $T_1^{-1}R_{\pi/3}T_2^{-1}R_{\pi/3}^{-1}=\mathcal{I}$ and $T_2^{-1}R_{\pi/3}T_1R_{\pi/3}^{-1}=\mathcal{I}$ are

$$\Delta_1\phi_{R_{\pi/3,p}}(r_1, r_2) = p'_4\pi + p_1r_2\pi,$$

$$\Delta_2\phi_{R_{\pi/3,p}}(r_1, r_2) = p'_5\pi + p_1(r_1 - r_2 - 1)\pi.$$

The solution to these equations is

$$\begin{aligned} \phi_{R_{\pi/3,p}}(r_1, r_2) &= \phi_{R_{\pi/3,p}}(0, 0) + p'_4\pi r_1 + p'_5\pi r_2 + p_1r_1r_2\pi \\ &\quad + \frac{1}{2}p_1r_2(r_2 - 1)\pi. \end{aligned}$$

Again we should not assume that $\phi_{R_{\pi/3,p}}(0, 0)$ are independent of sublattices index p .

Further constraint from $R_{\pi/3}\sigma R_{\pi/3}\sigma=\mathcal{I}$ is $p'_4=p'_5=0 \pmod 2$ and

$$2\phi_{R_{\pi/3,v}}(0, 0) = p_3\pi,$$

$$\phi_{R_{\pi/3,u}}(0, 0) + \phi_{R_{\pi/3,w}} = p_3\pi.$$

Therefore we have $\phi_{R_{\pi/3,v}}(0, 0)=p_3\pi/2$.

A similar constraint from $\sigma R_{\pi/3}\sigma R_{\pi/3}=\mathcal{I}$ is $p'_4=p'_5=0 \pmod 2$ and

$$2\phi_{R_{\pi/3,u}}(0, 0) = p_4\pi,$$

$$\phi_{R_{\pi/3,v}}(0, 0) + \phi_{R_{\pi/3,w}} = p_4\pi.$$

Combining with previous constraints on $\phi_{R_{\pi/3,p}}$ we conclude that $p_4 \equiv p_3 \pmod 2$ and $\phi_{R_{\pi/3,p}}=p_3\pi/2$.

Under the gauge transformation G_4 , the solution of $\phi_{R_{\pi/3}}$ transforms to

$$\begin{aligned} \phi_{R_{\pi/3,p}}(r_1, r_2) &\rightarrow \frac{p_3}{2}\pi + \pi + (p'_5 + 1)r_1\pi + p_1r_1r_2\pi \\ &\quad + \frac{1}{2}p_1r_2(r_2 - 1)\pi, \end{aligned}$$

while $\phi_{T_1,p}$, $\phi_{T_2,p}$, and $\phi_{\sigma,p}$ do not change. Therefore, we can always assume that $p'_5=0 \pmod 2$. The resulting constant π can be neglected because it is an IGG operation. Then we get the general solution (46d).

- ¹R. Coldea, D. A. Tennant, and Z. Tylczynski, Phys. Rev. B **68**, 134424 (2003).
- ²Y. Shimizu, K. Miyagawa, K. Kanoda, M. Maesato, and G. Saito, Phys. Rev. Lett. **91**, 107001 (2003).
- ³R. Masutomi, Y. Karaki, and H. Ishimoto, Phys. Rev. Lett. **92**, 025301 (2004).
- ⁴J. S. Helton, Y. S. Lee *et al.* (unpublished).
- ⁵G. Misguich, C. Lhuillier, B. Bernu, and C. Waldtmann, Phys. Rev. B **60**, 1064 (1999).
- ⁶S. Yunoki and S. Sorella, Phys. Rev. B **74**, 014408 (2006).
- ⁷M. Q. Weng, D. N. Sheng, Z. Y. Weng, and Robert J. Bursill, Phys. Rev. B **74**, 012407 (2006).
- ⁸Weihong Zheng, John O. Fjærestad, Rajiv R. P. Singh, Ross H. McKenzie, and Radu Coldea, Phys. Rev. Lett. **96**, 057201 (2006).
- ⁹X.-G. Wen, Phys. Lett. A **300**, 175 (2002).
- ¹⁰X.-G. Wen, Phys. Rev. B **65**, 165113 (2002).
- ¹¹Y. Zhou and X.-G. Wen, cond-mat/0210662 (unpublished).
- ¹²D. P. Arovas and A. Auerbach, Phys. Rev. B **38**, 316 (1988).
- ¹³N. Read and S. Sachdev, Phys. Rev. Lett. **66**, 1773 (1991).
- ¹⁴S. Sachdev and N. Read, Int. J. Mod. Phys. B **5**, 219 (1991).
- ¹⁵S. Sachdev, Phys. Rev. B **45**, 12377 (1992).
- ¹⁶S. V. Isakov, T. Senthil, and Y. B. Kim, Phys. Rev. B **72**, 174417 (2005).
- ¹⁷O. I. Motrunich, Phys. Rev. B **72**, 045105 (2005).
- ¹⁸C. J. Gazza and H. A. Ceccatto, J. Phys.: Condens. Matter **5**, L135 (1993).
- ¹⁹K. Lefmann and P. Hedegard, Phys. Rev. B **50**, 1074 (1994).
- ²⁰G. Misguich, B. Bernu, and C. Lhuillier, J. Low Temp. Phys. **110**, 327 (1998).
- ²¹Y. C. Chen, cond-mat/9312059 (unpublished).
- ²²Y. C. Chen and K. Xiu, Phys. Lett. A **181**, 373 (1993).
- ²³O. Tchernyshyov, R. Moessner, and S. L. Sondhi, Europhys. Lett. **73**, 278 (2006).
- ²⁴Th. Jolicoeur and J. C. Le Guillou, Phys. Rev. B **40**, 2727 (1989).
- ²⁵S. E. Korshunov, Phys. Rev. B **47**, 6165 (1993).
- ²⁶Th. Jolicoeur, E. Dagotto, E. Gagliano, and S. Bacci, Phys. Rev. B **42**, 4800 (1990).
- ²⁷A. V. Chubukov and Th. Jolicoeur, Phys. Rev. B **46**, 11137 (1992).
- ²⁸R. Deutscher and H. U. Everts, Z. Phys. B: Condens. Matter **93**, 77 (1993).
- ²⁹For larger values of next-neighbor coupling $\alpha > 0.31$, the location of the spinon minima jump to an incommensurate value, which we do not discuss here.
- ³⁰The expression for the permutation operator on four spin-1/2 can be written as $P_4 + \text{H.c.} = 4[(\mathbf{S}_i \cdot \mathbf{S}_j)(\mathbf{S}_k \cdot \mathbf{S}_l) - (\mathbf{S}_i \cdot \mathbf{S}_k)(\mathbf{S}_j \cdot \mathbf{S}_l) + (\mathbf{S}_i \cdot \mathbf{S}_l)(\mathbf{S}_j \cdot \mathbf{S}_k)] + (1/2)(\mathbf{S}_i + \mathbf{S}_j + \mathbf{S}_k + \mathbf{S}_l)^2 - (5/4)$.
- ³¹A. H. MacDonald, S. M. Girvin, and D. Yoshioka, Phys. Rev. B **37**, 9753 (1988).
- ³²D. J. Thouless, Proc. Phys. Soc. London **86**, 893 (1965).
- ³³C. H. Chung, J. B. Marston, and R. H. McKenzie, J. Phys.: Condens. Matter **13**, 5159 (2001).